

Molecular and Physicochemical Aspects of Local Anesthetics Acting on Nicotinic Acetylcholine Receptor-containing Membranes

Hugo R. Arias* and Michael P. Blanton

Departments of Pharmacology and Anesthesiology, School of Medicine, Texas Tech University Health Sciences Center, Lubbock, Texas 79430, USA; Department of Pharmaceutical Sciences, College of Pharmacy, Western University of Health Sciences, Pomona, California, 91766-1854, USA

Abstract: Local anesthetics inhibit the ion channel activity of nicotinic acetylcholine receptors in a noncompetitive fashion. This inhibitory action is ascribed to two possible inhibitory mechanisms: an open-channel-blocking mechanism and/or an allosteric process where the drug binds either to the closed channel or to other nonluminal sites, respectively.

INTRODUCTION

The most important pharmacological property of local anesthetics (LAs) is that they act on any nervous fiber of the nervous system inhibiting the action potentials responsible for nerve conduction. This effect is reversible at clinically-relevant concentrations. In other words, after a certain time, the nerve function is completely recovered without damage of the nerve fiber or the cell under treatment. Despite the vast clinical use of LAs, the molecular basis for local anesthesia began to be understood only 25 years ago. One of the first hypotheses to explain the pharmacological action of LAs incorporated the idea of nonspecific interaction with the lipid membrane. Today, it is known that the inhibitory action of LAs on nerve conduction is primarily due to the interaction of the drug with voltage-gated Na⁺ channels. Relevant aspects of the structure and function of voltage-gated Na⁺ channels on the nervous system can be found in several excellent reviews [1, 2]. Additional experimental evidence supports the conjecture that LAs may also act on several ion channels (e.g., K⁺ and Ca²⁺ channels), ion pumps, enzymes, and neurotransmitter-gated ion channel receptors (reviewed in [3]). For example, presynaptic Ca²⁺ channels and tachykinin type 1 receptors as well as nicotinic acetylcholine receptors (AChRs) are involved in the mechanism of spinal anesthesia. In addition, LAs decrease and eventually eliminate excitatory postsynaptic potentials [4].

Local anesthetics are able to cross the blood-brain barrier when administered systemically. At low (micromolar) concentrations, LAs produce loss of sensation (analgesia). At higher concentrations, they may provoke sedation or restlessness, tremulousness, dysphoria, convulsions, and ultimately, coma [5]. In addition, procaine and other LAs induce some behavioral effects that cannot be solely

explained by their actions on voltage-gated Na⁺ channels. All these data suggest that LAs produce additional pharmacological effects that may be mediated by the inhibition of ionotropic receptors. Among ionotropic receptors, the ligand-gated ion channel superfamily (LGICS) including muscle- and neuronal-type AChRs as well as type A and C γ -aminobutyric acid (GABA_AR and GABA_CR), glycine (GlyR), and type 3 5-hydroxytryptamine (5-HT₃R) receptors, is one of the best studied superfamilies that mediates excitatory (AChR and 5-HT₃R) as well as inhibitory (GABA_AR, GABA_CR, and GlyR) chemical transmission in the nervous system (reviewed in [6-8]). Particularly, LAs inhibit both muscle- and neuronal-type AChRs in a noncompetitive fashion, whereas they inhibit 5-HT₃R in a competitive manner (reviewed in [3]). Moreover, LAs inhibit GABA-induced currents on either 1 2, 1 2 s, or 4 2 s GABA_AR probably in a noncompetitive manner [9]. In this regard, experimental results indicate that LAs reduce the inhibitory currents induced by GABA or Gly in rat hippocampal neurons [10]. However, other results suggest that procaine does not inhibit GlyR expressed in *Xenopus* oocytes at concentrations up to 1 mM [11].

Since the introduction of (-)cocaine (the natural alkaloid of the leaves of the coca shrub *Erythroxylon coca*) into clinical practice in 1884, several behavioral effects including addiction and toxicity have been apparent. Cocaine abuse and addiction affects several millions of people annually in the world at an estimated cost of more than 100 billion dollars. The main target for the action of (-)cocaine has been elucidated. (-)Cocaine and related drugs inhibit the clearance of released monoamine neurotransmitters from the synaptic cleft by blocking several transporters (dopamine, serotonin, and norepinephrine transporters) [12]. Nevertheless, (-)cocaine also inhibits the AChR [13], the GlyR [14], and the GABA_AR from hippocampal neurons [15] in a noncompetitive fashion, and the 5-HT₃R in a competitive manner [16] (reviewed in [3]).

The aim of this mini-review is to describe the mechanisms by which LAs inhibit AChRs from peripheral

*Address correspondence to this author at the Department of Pharmaceutical Sciences, College of Pharmacy, Western University of Health Sciences, Pomona, California 91766-1854, USA; Phone: (909)-469-5581; Fax: (909)-469-5539; E-mail: huruar@pharmacology.ufl.edu

and central nervous systems as a model of the LA action on the LGICS. This work is also intended to explain how the conformational states of the AChR influence the pharmacological properties of LAs as well as to delineate the structural components of their binding sites.

BASIC STRUCTURE OF ACHRS

The muscle-type AChR is the archetype of the LGICS, which also includes the neuronal-type AChR as well as the GABA_AR, GABA_CR, GlyR, and 5-HT₃R (reviewed in [6-8]). Two additional ionotropic receptor superfamilies, i.e., the glutamate and the ATP receptor superfamily, are considered to be structurally different than the AChR LGICS (reviewed in [6, 8]). A scheme of the primary, tertiary, and quaternary structural features of the AChR LGICS is shown in Fig. (1). These receptors are considered a superfamily because a high degree of homology between the amino acid sequences of each receptor subunit exists [Fig. (1A)] (reviewed in [17]). For example, between neuronal and muscle AChR subunits sequence homologies of 48-70% have been found. However, an even higher homology is observed when key amino acid sequences are compared [e.g., ligand binding domains or the second transmembrane domain (M2)]. A second characteristic, shared by all LGICS members, is that each subunit can be divided in three portions: (1) an extracellular, (2) a transmembrane, and (3) a cytoplasmic portion [Fig. (1B)]. (1) The NH₂-terminal hydrophilic extracellular portion bears the neurotransmitter binding sites, several glycosylation sites, and the 15-residue Cys-loop between amino acids 128-142 corresponding to the *Torpedo* 1 subunit [17]. (2) The transmembrane domain of each subunit is formed by four highly hydrophobic segments designated M1, M2, M3, and M4 [Fig. (1B)]. These membrane-spanning helices have a dimension of 30-35 Å (40 Å including the phospholipid headgroup portion). The domains M1, M2, and M3 are separated from each other by short hydrophilic stretches. The hydrophilic faces of the five M2 segments, one from each receptor subunit, form the walls of the ion channel. The ion channels from GABA_AR, GABA_CR, and GlyRs, are permeable to anions (e.g., Cl⁻), whereas the ion channels from 5-HT₃R and AChRs allow the passage of cations (e.g., Na⁺, K⁺, and Ca²⁺). The M1, M3, and especially the M4 transmembrane domain of the AChR, and probably from other LGICS members as well, are in contact with the lipid membrane. (3) The hydrophilic cytoplasmic domain, which is approximately four-fold smaller than the NH₂-terminal domain, is located between segments M3 and M4. The M4 domain orientates the COOH-terminus to the synaptic side of the membrane. The large cytoplasmic domains of these receptors carry several phosphorylation sites (reviewed in [18]).

Information on the structure of LGICS members has come predominantly from studies of the muscle-type AChR. The muscle-type AChR is a heteromeric membrane-embedded protein formed by four subunits in the stoichiometric ratio of $\alpha_2\beta\gamma$ (embryonic) or $\alpha_2\beta\delta$ (adult). The muscle-type AChR from electric fish such as *Torpedo* and *Electrophorus* species is most closely related to the embryonic form. Based upon the presence of two

adjacent cysteines at or close to position 192 and 193 of the *Torpedo* subunit, which participate in cholinergic ligand binding, the neuronal-type AChR subunit classes are designated (contain both cysteines) and non- or (do not contain those cysteines). To date, nine subunits (2 to 10) and three subunits (2 to 4) have been identified in vertebrates (reviewed in [6, 7]). The α and β subunits of the muscle-type AChR are designated as α_1 and β_1 . Additionally, spliced forms of both α_2 [19] and β_3 [20] subunits exist.

By homology with the muscle-type AChR, neuronal AChRs are also believed to form oligomers composed of five subunits [21]. Depending on the kind of tissue involved, AChRs can be combined in several subunit arrangements. There is an evidence supporting the existence of neuronal receptors containing one, two, three, or four different subunits. Among homomeric receptors, there are α_7 , α_8 , and α_9 receptors (reviewed in [3, 7, 23]). The α_7 subunit has been shown to assemble with either the α_8 [24] or the α_3 [25] chain, whereas the α_9 subunit co-assembles with the α_{10} chain [22]. Among heteromeric receptors, the existence of $\alpha_2\alpha_2$, $\alpha_3\alpha_2$, $\alpha_4\alpha_2$, $\alpha_2\alpha_4$, $\alpha_3\alpha_4$, $\alpha_6\alpha_4$, $\alpha_6\alpha_2$, and $\alpha_4\alpha_4$ receptors have been confirmed in different species. The $\alpha_4\alpha_2$ combination, one of the most prominent subtypes found in vertebrate brains, is believed to have the stoichiometry (α_4)₂(α_2)₃ [21]. In addition, combinations of three different subunits forming receptors $\alpha_3\alpha_5\alpha_2$, $\alpha_3\alpha_5\alpha_4$, $\alpha_4\alpha_5\alpha_2$, $\alpha_3\alpha_6\alpha_4$, $\alpha_3\alpha_4\alpha_5$, and $\alpha_3\alpha_4\alpha_2$ have been detected in distinct species. Finally, the organization $\alpha_3\alpha_2\alpha_4\alpha_5$ is proposed to exist in chicken ciliary ganglion neurons and in some human neuroblastoma cell lines [26]. The existence of a high number of structurally-distinct receptor entities, each with different ligand sensitivities, suggests that each AChR class may have a distinct physiological function. Interestingly, whereas in heteromeric receptors two agonist/competitive antagonist binding sites have been found, in homomeric receptors up to five sites may exist [see Fig (1C)] [27].

Although the muscle-type AChR is believed to have a $\alpha_2\beta\gamma$ subunit arrangement (reviewed in [3, 6-8]), there is no direct evidence indicating the arrangement of neuronal subunits around the ion channel. The organization $\alpha_4\alpha_2\alpha_4\alpha_2\alpha_2$ has been suggested for the predominant AChR subtype present in the brain and the arrangement $\alpha_3\alpha_5\alpha_2\alpha_3$ (where α_2 may be only α_4 or alternatively α_2 or α_4) is presumed to exist in chicken ciliary ganglion neurons (reviewed in [3, 6, 7]).

Electron microscopic analysis has helped elucidate the overall structure of the muscle-type AChR (reviewed in [28]). Viewed from the synaptic cleft, the AChR appears as a rosette 70-80 Å in diameter with a central depression 25 Å wide. The five subunits are arranged pseudo-symmetrically around an axis that passes through the ion pore, perpendicular to the plane of the lipid membrane. The observed rosette is formed by the extracellular hydrophilic domain of the receptor containing both the NH₂- and the COOH-terminal [Fig. (1C)]. The NH₂-terminus of each subunit is formed by approximately 210 amino acids, protrudes ~60 Å toward the synaptic cleft. The observed

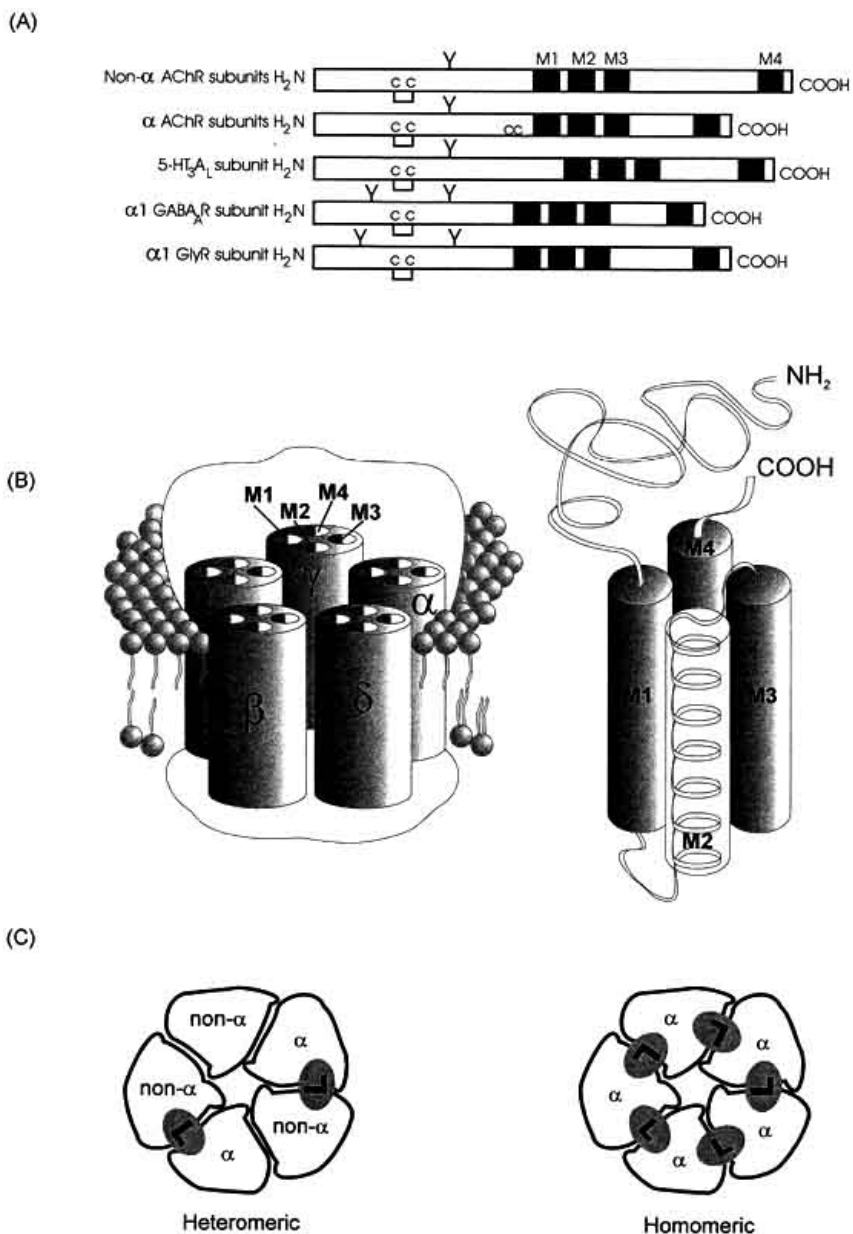


Fig. (1). Schematic representation of the structural organization of the AChR LGICS members. (A) Schematic illustration of the primary sequence of several subunits from members of the LGICS which includes the (1-10) and non- (1-4, , , and) subunits of the AChR, the A subunit of the 5-HT₃R, the α 1 subunit from the GABA_AR, and the α 1 subunit from the GlyR. M1-M4, transmembrane domains; C-C, Cys-Cys bridge found in the ion-channel superfamily (homologous to Cys¹²⁸ and Cys¹⁴⁸ of the α 1 AChR subunit); CC, Cys-Cys pair found in the subunits from both muscle- and neuronal-type AChRs (corresponding to Cys¹⁹²-Cys¹⁹³ from the α 1 AChR subunit); , oligosaccharide groups. (B) Diagram of the tertiary and quaternary organization of the AChR as an example for other members of the LGICS. Each AChR subunit includes: (1) a long NH₂-terminal hydrophilic extracellular region; (2) four highly hydrophobic domains named M1, M2, M3, and M4. It is postulated that the intrinsic ion channel is composed by five M2 segments, one from each subunit. Moreover, M1-M2 and M2-M3 are connected by minor hydrophilic stretches; and (3) a major hydrophilic segment facing the cytoplasm. Additionally, the M4 domain orientates the COOH-terminus to the synaptic side of the membrane. (C) Schematic representation of the oligomeric organization of AChR as an example for other members of the LGICS. The hypothetical pentameric AChR is formed by two α subunits and three non- α chains. The two ligand binding sites (L) are located at the interfaces of one α subunit and one non- α chain. For instance, the muscle-type AChR presents a high-affinity acetylcholine binding site at the α subunit interface and another low-affinity acetylcholine locus at the α subunit interface (but see the review by Unwin [28]). Regarding homomeric AChRs (e.g., 7-9), up to five ligand binding sites may exist.

central depression is the vestibule, a large region located on the extracellular domain of the AChR connecting the extracellular medium with the ion channel proper. The wall of the ion pore is formed by the M2 transmembrane segment from each subunit. The other transmembrane segments of the muscle-type AChR, M1, M3, and M4, are believed to be in closer contact with the lipid phase (reviewed in [3, 29]). Particularly, M4, the most hydrophobic segment, is also the least conserved transmembrane segment. The M1 and M3 domains are considered important for AChR assembly and channel gating, respectively. The transmembrane domain from each muscle-type AChR subunit is formed by 19-27 residues, giving a calculated length of about 40 Å if the sequence is assumed to form α -helix [Fig. (1B)]. Although the transmembrane sequences have traditionally been considered α -helical [99], recent studies have suggested the existence of a α -helical/ β -strand mixed secondary structure (reviewed in [6, 7]). Therefore, the secondary structure of LGICS membrane-spanning segments remains unresolved.

Regarding the surface of the AChR in intimate contact with the lipid membrane, two lipid binding regions have been identified: the annular lipid domain and the nonannular lipid domain [30]. The annular lipid domain is surrounded by a belt of 45 lipid molecules abutting the intramembraneous perimeter of the AChR. Although the structural details for the nonannular lipid binding sites are unknown, these sites have been proposed to be located at the intramolecular interfaces of the five subunits and/or at the interstices of the four transmembrane domains [30, 31].

The intracellular hydrophilic domain of the AChR, the major cytoplasmic loop, measures 15-20 Å wide and is composed of, 109 to 142 amino acids [Fig. (1B)] depending on the subunit. Regarding the muscle-type AChR, this loop contains the region that interact non-covalently with the peripheral membrane protein rapsyn, originally called 43 kDa protein. This protein functions in receptor clustering and receptor-cytoskeleton communication [32]. On the *Torpedo* subunit, an additional Cys residue forming a disulfide bridge between two AChR protein monomers, each with a molecular mass M_r 290 kDa, was found. However, the exact physiological rationale for the existence of AChR dimers in electrocytes (typical cells of electric organs from *Torpedo* and *Electrophorus* species) has not been elucidated.

The structure of the ion channel has been studied using different methodological approaches including photoaffinity labeling and site-directed mutagenesis in combination with electrophysiological methods. For example, studies determining the photo-crosslinking extent of either radiolabeled or photoactivatable noncompetitive inhibitor (NCI) derivatives with specific photoreactive groups have given rise to an important conclusion: the structure of the ion channel wall is principally formed by the transmembrane M2 domain of each AChR subunit. In a simplistic manner, the ion channel can be considered to be similar to a cylindrical tube with a diameter of 20-25 Å that protrudes along the lipid bilayer (40 Å height, including the phospholipid headgroup region) [see Fig. (1B)]. Although the structural characteristics of the transmembrane portion of the channel have not been resolved in detail, the narrowest portion of the cylinder is considered to have a diameter of

7 Å [28]. The observed diameter is large enough to allow the passage of Na^+ or K^+ cations with a single hydration shell. In addition, the length of this particular region has been estimated by potential streaming measurements to be 3-6 Å long [33], approximately the extension of one α -helical turn. This evidence is in agreement with electron microscopic image analyses at 4.6 Å resolution indicating that the closed ion channel has a narrow strip of density no longer than two rings of side-chains thick (reviewed in [28]). This specific portion of the ion channel, the so-called gate, has been positioned close to either the middle (reviewed in [28]) or the cytoplasmic end of the ion channel in the resting state [34]. Interestingly, the localization of the gate in either the transient (I) [35] or the stable (D) [36] desensitized state [see Fig. (2)] is postulated to be different from the gate in the resting state. In comparison with other members of the LGICS, the dimensions of the narrowest part of the ion channel follow the sequence: GlyR < GABA_AR < 5-HT₃R AChR (reviewed in [29]).

Additional evidence indicates that there are two categories of domains within the AChR channel (reviewed in [3, 7, 29]). An uncharged domain that is formed by a series of different rings vectorially disposed from the extracellular to the intracellular channel portion in the order: valine ring (position 13), leucine ring (position 9), serine ring (position 6), and threonine ring (position 2). In turn, this uncharged portion is framed by two negatively-charged domains: an anionic ring located at the extracellular portion of the channel [the outer ring (position 20)] and two more anionic rings located near the cytoplasmic portion of the channel [the intermediate ring (position -2) and the inner ring (position -5)].

BASIC FUNCTION OF ACHRS

Nicotinic acetylcholine receptors, similar to other members of the LGICS, present a very simple repertoire of functional properties. The AChR recognizes the neurotransmitter acetylcholine (ACh), and upon its binding, the intrinsically-coupled ion channel is opened, allowing cations to cross the lipid membrane (Na^+ and Ca^{2+} enter into the cell whereas K^+ exits the cell). This concentration change produces membrane depolarization. The depolarization of the membrane provokes specific physiological responses in the cell. For instance, if the muscle membrane depolarization is large enough, an action potential is elicited. This action potential propagates from the neuromuscular junction all over the muscle fiber. During the propagating action potential the release of Ca^{2+} ions from intracellular stores in the muscle is stimulated. The final response in the muscle is the contraction of its myofibrils. Nevertheless, in neurons, the excitatory signal provided by the activation of the cation channel is summated with other signals, including inhibitory signals such as those provided by the activation of either GABA_ARs or GlyRs, and subsequently re-directed to another neuron or to an endocrine gland cell. The chemo-electrical transduction process also produces transference of frequency-encoded information between neurons, with the concomitant significance on memory and learning processes.

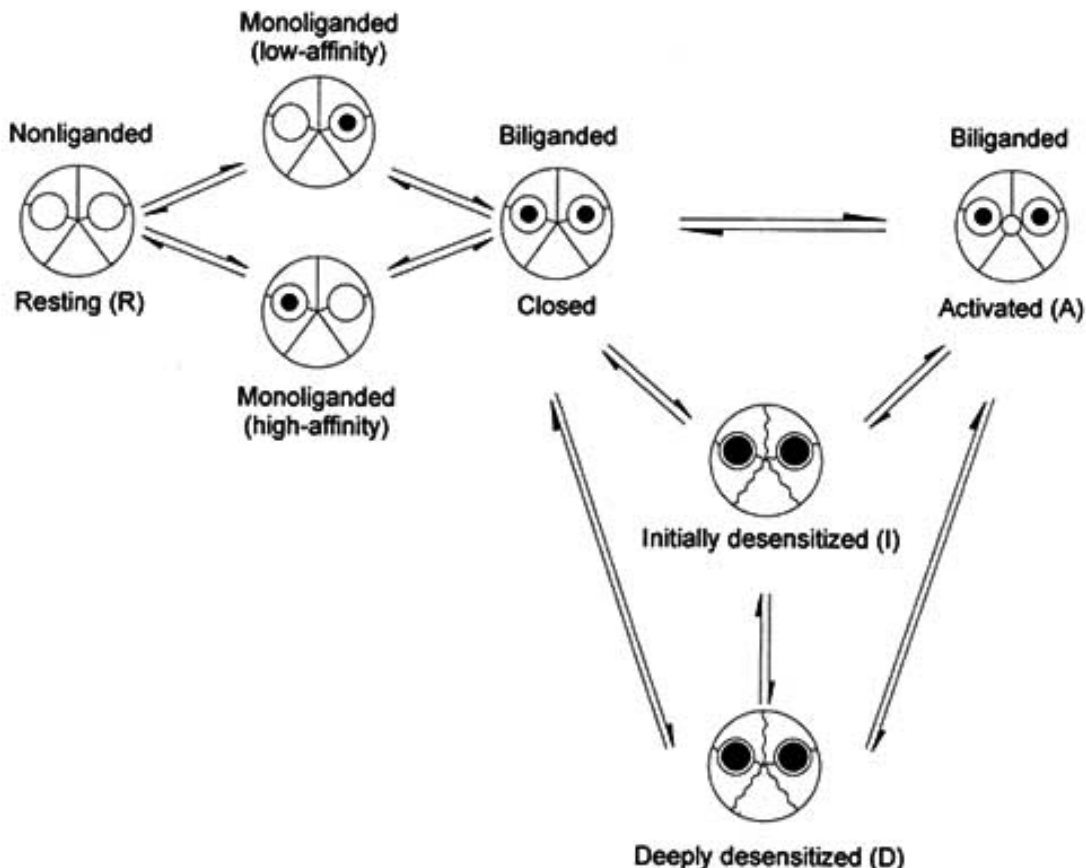


Fig. (2). Diagram showing the dynamic of the multiple conformational states of the AChR. In the absence of the neurotransmitter acetylcholine (ACh), the AChR is in the resting (R) state, a conformational state where the ion channel is closed. The binding of one ACh molecule (showed here as black circles) to its respective high- or low-affinity site produces monoliganded (closed) receptors. The closed ion channel can be opened upon binding of two ACh molecules to the AChR (biliganded receptors). This active (A) state presents low affinity for agonists (K_d 's from 10 μM to 1 mM) [showed here as a loosed interaction between ACh molecules (i.e., black circles) and the AChR]. The transition from the R to the A state is a fast process which proceeds in the microsecond-to-millisecond time regime. In the prolonged presence of agonists, the AChR becomes refractive to the agonist pharmacological action and thus, to the activation of its ion channel. In the *Torpedo* AChR there exists two refractive closed ion channel states, the initially desensitized (I) and the deeply desensitized (D) state. Both states show high affinity for agonists and some antagonists (K_d 's from 10 nM to 1 μM) [showed here as a tight interaction between ACh molecules (i.e., black circles) and the AChR]. The transition from the A to the I state is a slow process which is produced in the 1-100 ms time range. Additionally, the transition from the A to the D state has a much slower time course (in the second to minute time frame).

Each AChR subtype presents a distinct specificity for different agonists and competitive antagonists. For instance, neuronal-type AChRs can be divided in two main groups: those that bind the competitive antagonist α -bungarotoxin (α -BTx) in the nanomolar concentration range and agonists (e.g., nicotine) in the micromolar concentration range, and those that bind agonists with nanomolar affinities but do not bind α -BTx (reviewed in [37]). Among those that bind α -BTx with high affinity, include α 7-9 homomeric AChRs. The α 7 subunit accounts for most of the high-affinity α -BTx binding sites present in both the central and peripheral nervous systems.

Although both muscle- and neuronal-type AChRs present the same basic functional attributes, two properties have been assigned as representative of neuronal AChRs. Neuronal-type AChRs have higher Ca^{2+} permeability (P). For example, the $P_{\text{Ca}}/P_{\text{Na}}$ ratio ranges from 1.1 (for the

α 4 subtype) to >10 (for the α 7 subtype) (reviewed in [38]). Additionally, the positive modulation of the opening probability of the neuronal-type ion channel is mediated by external Ca^{2+} levels (reviewed in [23, 37]). The observed high Ca^{2+} permeability through α 7 receptors ($P_{\text{Ca}}/P_{\text{Na}}$ 20) may be important for physiological functions such as regulation of both the GABA_A R and the N-methyl-D-aspartate-type glutamate receptors, induction of long-term potentiation in neurons (reviewed in [37]), neurite retraction [39], and survival of spinal cord motoneurons [40]. In addition, presynaptic neuronal AChRs may be involved in the release of neurotransmitters such as ACh, glutamate, norepinephrine, dopamine, 5-HT, or GABA (reviewed in [41, 42]).

All these physiologically-relevant AChR properties are triggered by the binding of the neurotransmitter ACh (reviewed in [7]). First, one ACh molecule binds to its

respective high- or low-affinity site, producing monoliganded receptors. Next, a second ACh molecule binds the monoliganded receptor to form the biliganded receptor. The biliganded receptor remains closed but after a certain time, the receptor protein undergoes a conformational change that opens the ion pore.

Several lines of experimental evidence suggest that the AChR may exist in a minimum of four interconvertible states (reviewed in [5-7]). Figure (2) shows a diagram indicating four receptor states. In the absence of agonists, most *Torpedo* receptors (80%) are in the resting state (R). Reciprocally, 20% of receptors are in the desensitized state (D). In the presence of agonists, the biliganded receptor is activated (A) in the microsecond to millisecond range. The A state represents an open ion channel with low affinity for agonists [apparent dissociation constant (K_d) between 10 μ M and 1 mM]. In the prolonged presence of agonists, the activated receptor converts to a transient desensitized state (I) in the 1-100 ms timescale (fast-onset) and then to a more stable desensitized state (D) in the second to minutes timeframe (slow-onset). Both I and D states are refractory to the pharmacological action of agonists, and the ion channel

remains closed. In addition, both the I and D states have high affinity for agonists and some antagonists (apparent K_d ranging from about 10 nM to 10 μ M). After the dissociation of agonist molecules from their binding sites, AChRs in the D state predominantly isomerize directly to the R state and this recovery process is slower than the forward rate. Thus, the physiological role of the desensitization process in the LGICS has so far not been determined. However, under some pathological conditions the importance of this course of action becomes apparent (reviewed in [43]). For instance, activation and/or subsequent desensitization of neuronal AChR subtypes are believed to underlie behavioral addiction to nicotine (reviewed in [44]).

STRUCTURAL FEATURES OF LOCAL ANESTHETIC MOLECULES

Chemically, LAs can be considered as aromatic amines (reviewed in [45]). Most known LAs are amphiphilic molecules composed of a lipophilic moiety (aromatic group) and a positively-charged or a protonatable amine group. The hydrophilic and hydrophobic portions are separated by an

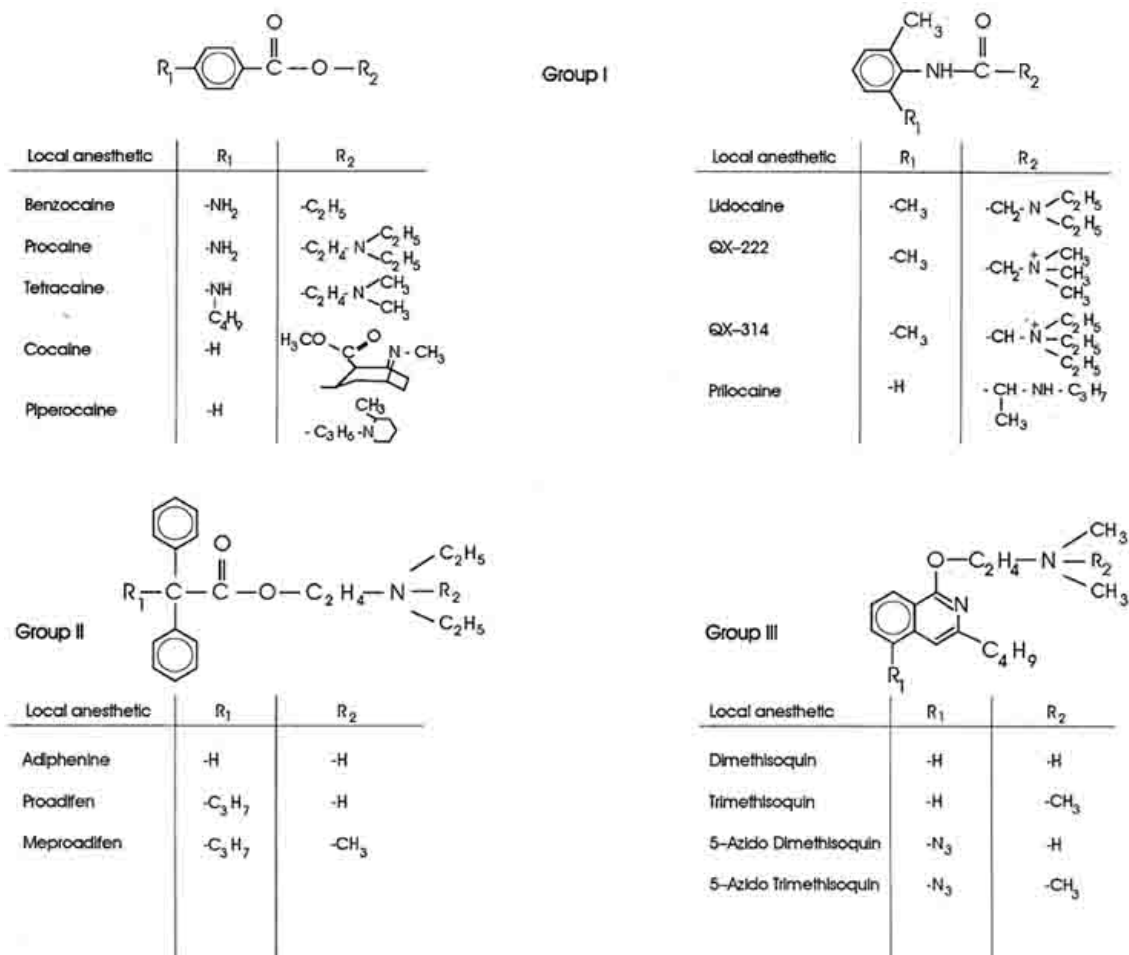


Fig. (3). Molecular structures of local anesthetics tested on different AChR types.

aminobenzoate) and its spin-labeled analogue Benzocaine-SL [compound I in Fig. (4)]. Examples of quaternary (or permanently-charged) LAs are the lidocaine derivatives QX-222 (trimethylamine derivative) QX-314 (triethylamine derivative), meproadifen, trimethisoquin, bupivacaine methiodide, and the spin-labeled analogues VI⁺/Me and C6SL-MeI [see structures in Fig. (4)]. The remaining LAs have tertiary and secondary amine groups. Concerning tertiary LAs, the charge is dependent on the pH of the medium (reviewed in [3, 45]).

MOLECULAR MECHANISMS OF LOCAL ANESTHETIC INHIBITION OF THE ACHR

The early use of electrophysiological techniques such as voltage jump relaxation and agonist-induced noise spectra analysis demonstrated that LAs depress synaptic transmission by inhibiting the AChR (reviewed in [3]).

These and subsequent studies on single-activated ion channels from both muscle- and neuronal-type AChRs supported the notion that the pharmacological action of LAs is elicited upon binding to the ion channel. Like other NCIs (reviewed in [29]), LAs exert their blocking action on AChRs reducing the duration of ion channel open time without changing maximal agonist binding. However, the mechanism of channel inhibition is still a matter of controversy. Experimental evidence supports the idea of channel blocking by a steric mechanism in which the drug enters into the lumen channel, binds and plugs it like a cork in a bottleneck. However, LA binding to its site is not static and uniform. As a consequence of thermal energy fluctuations, both the ligand and the more mobile part of the macromolecule continuously and randomly move. Thus, a LA molecule may reach its specific site, occupy it, and then depart more or less rapidly from it. In other words, there exists a true equilibrium between the unbound and the bound species. In fact, this has been demonstrated for QX-

Table 1. Voltage Sensitivity and Apparent Voltage-sensitive Location of Local Anesthetics on Both Muscle- and Neuronal-type AChR ion Channels

Local Anesthetic	AChR Source	Voltage Sensitivity ^a mV	Apparent Voltage-Sensitive Location	References
QX-222	Parasympathetic neurons from Rat intracardiac ganglia	62	0.40	[4]
	Rat 4 2 expressed in <i>Xenopus</i> oocytes	26	0.92	[48]
	Mouse 1 ₂ 1 expressed in <i>Xenopus</i> oocytes	39.1	0.65-0.75	[51]
	Mouse 1 ₂ 1 ₂ expressed in <i>Xenopus</i> oocytes	39.5	0.65-0.75	
	Mouse 1 ₂ 1 expressed in <i>Xenopus</i> oocytes		0.65-0.75	[52]
	Mouse 1 ₂ 1	-	0.70-0.80	[53]
	Rat muscle	64	-	[60]
	Frog muscle (junctional)	50	-	[61]
	Frog muscle (extrajunctional)	32	0.78	[47]
QX-314	BC ₃ H-1 cells	42	-	[62]
	Rat muscle myoballs	-	0.72	[54]
Procaine	Parasympathetic neurons from Rat intracardiac ganglia	122	0.20	[4]
	Frog muscle (junctional)	50	0.50	[50]
	Frog sartorius muscle	86	0.30	[55]
	Bovine adrenal chromaffin cells	55	-	[63]
(-)Cocaine	Rat 3 4 expressed in <i>Xenopus</i> oocytes	34	-	[49]
	Rat 3 2 (2Val ²⁵³ Phe) expressed in <i>Xenopus</i> oocytes	45	-	
	Rat 4 2 expressed in <i>Xenopus</i> oocytes	90	-	
	Frog muscle	-	0.18	[56]
Bupivacaine	Mouse myoballs	-	0.18	[57]
	<i>Rana pipiens</i> muscle	-	0.05-0.11	[58]
Piperocaine Methiodide	Frog sartorius muscle	-	0.06	[59]

^a The voltage sensitivity of LAs is determined by the e-fold (2.718-fold) change in the apparent IC₅₀ (or K_i) for a given variation (hyperpolarization) in membrane potential (mV).

222, the archetype of quaternary LAs acting on the AChR [47]. Single channel analyses showed that the presence of QX-222 causes the agonist-evoked current to flicker. This flickering represents the repeatedly action of LA binding (block) and dissociation to (or from) open channels, appearing as bursts of briefer than normal openings.

One of the earliest pieces of evidence supporting a steric mode of action was provided by voltage-clamp experiments where the inhibitory action of LAs, like other NCIs, was shown to be modulated by membrane potential changes (reviewed in [3, 29]). Although almost all LAs are considered to be voltage-sensitive, uncharged LAs (e.g., benzocaine and dibucaine; [46]) and the unprotonated forms of all other LAs are voltage-insensitive because they cannot be expelled from the channel at positive potentials. In most cases, the inhibitory effect of quaternary LAs is more sensitive to membrane potential than the effect elicited by tertiary LAs. The potentiation of LA inhibition of transient agonist-evoked currents by membrane hyperpolarization can be quantified by calculating the e-fold (2.718-fold) change in the apparent IC_{50} value of the LA under study. The voltage sensitivity for several LAs is shown in Table 1. In general, e-fold change values range from 26 mV for QX-222 in the neuronal $\alpha 2$ subtype [48] to 122 mV for procaine in parasympathetic neurons from rat intracardiac ganglia [4]. In addition, the observed values depend on both the LA and the AChR type. For instance, considering the same receptor class (e.g., rat $\alpha 2$ expressed in *Xenopus* oocytes), the e-fold change is 26 mV for QX-222 [48] or 90 mV for (-)cocaine [49]; whereas, considering the same LA (e.g., procaine) the values range from 50 [50] to 122 mV [4] for the muscle- and neuronal-type AChR, respectively. Taking into account the apparent voltage-sensitive location of LAs (see Table 1), the main conclusion is that LAs bind at a site within the electrical field, presumably the ion channel. More specifically, the binding site for QX-222 [4, 47, 48, 51-53] and QX-314 [54] may be located closer to the cytoplasmic side of the receptor, whereas the procaine locus is near the middle of the ion channel [4, 50, 55], and the binding sites for (-)cocaine [56], bupivacaine [57, 58], and piperocaine methiodide [59] are much closer to the extracellular side of the receptor. Nevertheless, the QX-222 site location in the AChR ion channel from parasympathetic neurons [4] seems to be more external than in both $\beta 1$ [47, 51-53] and $\alpha 2$ [48] subtypes.

On the basis of the experimental results described above and additional observations, the open-channel-blocking mechanism was postulated (reviewed in [3]). The scheme of Fig. (5) shows the basic steps that account for the open-channel-blocking mechanism. In the same figure, the allosteric inhibitory process, which is developed below, is also shown. Although a great body of information supports the existence of an open-channel-blocking mechanism, deviations of this simple mechanism have been observed. For example, a cyclic model where the anesthetic binds to closed channels has also been suggested [50]. This evidence is in accord with the existence of an allosteric inhibitory mechanism. The interaction between the closed [resting, monoliganded, or biliganded; see Fig. (2)] receptor and the ligand induces a conformational change on the protein preventing the opening of the ion channel and thus,

depressing ion flux activity. An approach that allows us to distinguish between the two open-channel-blocking and allosteric mechanisms is determining the effect of LAs on both apparent channel opening and closing rate constants. If the open-channel-blocking is the main inhibitory mechanism, then, only the apparent rate constant for channel closing should decrease as LA concentration is increased. On the contrary, if the allosteric mechanism is the principal mechanism of inhibition, then, both apparent rate constants should decrease as the LA concentration increases. Utilizing fast kinetic techniques, Hess and co-workers, demonstrated that both apparent channel opening and closing rate constants decreased with increasing procaine concentrations, suggesting the existence of a regulatory site to which the LA binds before the channel opens [64]. The conclusions of these studies are summarized in the scheme of Fig. (5). The allosteric mechanism establishes that LAs bind to a regulatory site on the AChR, inhibit channel opening, and decrease the AChR in the open state by a slow course that converts to receptors in the active form. In other words, procaine preferably binds to the closed channel (A_nR) forming the A_nRL complex and thus, inhibiting ion flux ($A_nR'L$) [see Fig. (5)]. In addition, tetracaine prefers the AChR in the resting state (R) forming the RL complex which reduces the conversion to the open channel (R'L). In the case of (-)cocaine, the rate of channel opening is not affected but the rate of channel closing is slightly (1.5-fold) increased [13]. The affinity of (-)cocaine for the open channel is 6-fold lower than that in the closed state (see Table 2). Nevertheless, with the dissociative anesthetic dizocilpine (a drug that has been used as a palliative on cocaine addiction) the closing rate constant increases with increasing inhibitor concentration, whereas the opening rate constant does not change [65]. These results are consistent with a two step mechanism: first, (-)cocaine or dizocilpine rapidly binds to a regulatory site on the closed channel (A_nR) without affecting ion channel properties. In this regard, the ion channel might open with the drug bound (A_nR^*L). Next, the AChR-bound inhibitor complex (A_nRL) is slowly ($t_{1/2} = 70$ ms) transformed to a non-conducting state [$A_nR'L$; see Fig. (5)]. More recent studies on the characterization of the dizocilpine binding site suggest that this site is located close to the quinacrine locus probably at a nonluminal domain [66]. Alternatively, LAs may also bind to open channels with the subsequent inhibition of ion flux. In particular, the quaternary LA QX-222 binds preferably to the open channel (A_nR^*) forming the A_nR^*L complex and thus, inhibiting ion flux ($A_nR'L$) [see Fig. (5)]. Probably, this latter mechanism is more important for quaternary than for tertiary LAs. Since the channel should be open before the LA inhibits it, the short time that the channel remains open will be enough for the initiation of the membrane depolarization process. Thus, the physiological implication of this mechanism is not obvious. The allosteric mechanism seems to be more significant for the inhibitory action of tertiary LAs. The existence of this regulatory mechanism may be of physiological relevance: the binding of an inhibitor to its regulatory site before the channel is open may ultimately preclude the signal transmission between cells. In turn, this perturbation of neurotransmission might be involved, at least partially, with the behavioral effects observed for (-)cocaine and their analogues including LAs. In this regard,

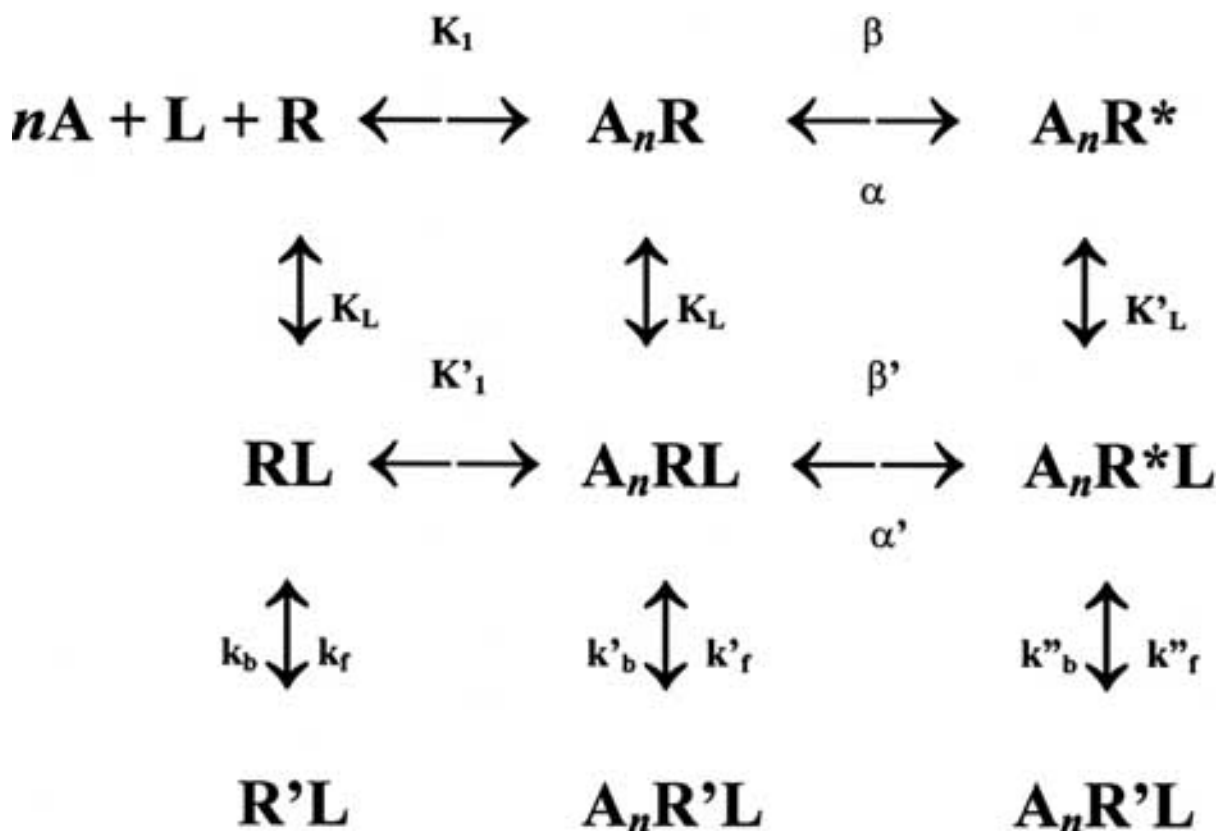


Fig. (5). Activation and alternative (open-channel-blocking and allosteric) mechanisms for the local anesthetic inhibition of the AChR (modified from [13, 64, 65]). The reaction of activation is initiated when n agonist molecules (nA) bind to the AChR (R) in the resting (closed but activatable) state. For heteromeric AChRs, two agonist molecules ($n=2$) should bind to the receptor to allow the opening of the ion channel. For homomeric AChRs (e.g., 7- 9), up to five agonist molecules ($n=5$) may putatively bind to the AChR. The apparent dissociation constants K_1 and K'_1 represent the equivalent binding steps for nA in the absence or in the presence of local anesthetic (L), respectively. The binding reactions finally lead to the closed receptor-ligand complex A_nR (in the absence of LA). Upon binding, several protein transitions result. The ion channel is open (A_nR^*) in the microsecond-millisecond time regime. The transitions between closed and open channels is characterized by rate constants for channel opening (α) and closing (β). In the presence of LAs , both open (A_nR^*) and closed (R and A_nR) AChRs form the respective inhibitor-AChR complexes (A_nR^*L , RL , and A_nRL). In particular, the quaternary LA QX-222 binds preferably to the open channel (A_nR^*) forming the A_nR^*L complex and thus, inhibiting the ion flux (A_nR^*L). In addition, procaine and cocaine preferably bind to the closed channel (A_nR) forming the A_nRL complex and thus, inhibiting ion flux ($A_nR'L$). Instead, dizocilpine binds to the closed channel (A_nR) forming the A_nRL complex, but allowing the channel to be open (A_nR^*L). The equilibrium between A_nR^*L and A_nRL is characterized by rate constants α' and β' , respectively. In the presence of agonists or LAs , the receptor is rapidly (~ 100 ms) converted to the desensitized form (not shown here for simplicity). K_L and K'_L are the apparent LA K_{dS} for the closed and open forms of the ion channel, respectively. k_f and k_b are the overall rate constants for the $R'L$ (inhibited) complex formation, whereas k'_f and k'_b , and k''_f and k''_b are the overall rate constants for the $A_nR'L$ (inhibited) complex formation.

the search for alternative drugs to alleviate the consequences of abusive use of cocaine and other derivatives should take into account a molecular structure that may compete for the cocaine site without producing its inhibitory effect.

LOW-AFFINITY LOCAL ANESTHETIC BINDING SITES

Experimental evidence for the localization of LA binding sites on the AChR was obtained using a wide range of different techniques from the fields of spectroscopy, electrophysiology, biochemistry, pharmacology, and molecular biology. On the basis of equilibrium binding

experiments, a population of 10-30 binding sites for different NCIs was found on the AChR [67] (reviewed in [3, 29]). These sites present low affinity and are not sensitive to displacement by the pharmacological action of the high-affinity NCI histrionicotoxin (HTX). In this regard, LAs with these pharmacological features correspond to the group of low-affinity NCIs. The apparent K_{dS} for these LAs range from 39 μM for trimethisoquin [67] to 500 μM for benzocaine [68] (Table 2). However, more recent data indicate the existence of approximately four displaceable low-affinity NCI binding sites for dissociative anesthetics such as phencyclidine (PCP) [69] and dizocilpine [66], respectively.

Table 2. Local Anesthetic Preference for the Different Conformational States of the AChR

Local Anesthetic	Conformational State				References
	Resting K _d , μM	Desensitized K _d , μM	Open IC ₅₀ , μM	Membrane voltage, mV	
Group I					
Procaine	790 ± 80 (<i>T. ocellata</i>)	690 ± 120 (<i>T. ocellata</i>)		0	[114]
			88 ± 10 (1 ₂ 1 ₁ ; BC ₃ H-1)	-60	[64]
			110 ± 50 (rate constant for channel closing)	-60	
			40 ± 60 (rate constant for channel opening)	-60	
			15 ± 2 (1 ₂ 1 ₁ ; Mouse)	-90	[99]
			50 ± 9 (1 ₂ 1 ₁ ; Mouse)	-45	
			100 (1 ₂ 1 ₁ ; Mouse)	-40	[115]
			70 (1 ₂ 1 ₁ ; Mouse)	-80/-90	[116]
			35 (CCh-evoked catecholamine secretion)	0	[63]
80 (²² Na ⁺ influx in chromaffin cells)	0				
100 (²² Na ⁺ influx in PC-12 cells)	0	[117]			
2.8 (Parasympathetic neurons)	-80	[4]			
40 ± 3 (⁸⁶ Rb ⁺ influx in <i>T. californica</i> vesicles)	-25	[118]			
Tetracaine	0.5 ± 0.1 (<i>T. californica</i>) 2.2	29 ± 7 (<i>T. californica</i>) 43		0 0	[70]
			1 (1 ₂ 1 ₁ ; electrocyte) 38 (1 ₂ 1 ₁ ; BC ₃ H-1)	-60 -80	[96]
	0.31 ± 0.03 (<i>T. californica</i>)			0	[97]
(-)Cocaine	50 ± 10 (BC ₃ H-1)		300 ± 70 (BC ₃ H-1)	-90	[13]
			6-14 (Cs ⁺ influx in <i>E. electricus</i> vesicles)	0 0	[118]
			58 (Cs ⁺ influx in <i>T. californica</i> vesicles)		
			10 (²² Na ⁺ influx in PC-12 cells)	0	[117]
			17 (Frog sartorius muscle)	-100	[56]
			4.4-6.9 (4 2; Rat)	-70	[112]
			22.0-42.3 (3 2; Rat)	-70	
			2 (4 4; Rat)	-50	[49]
			6 ± 1 (3 4; Rat)	-50	
16 ± 4 (2 4; Rat)	-50				
15 ± 1 (4 2; Rat)	-50				

(Table 2). contd.....

Local Anesthetic	Conformational State			Membrane voltage, mV	References
	Resting K_D , μ M	Desensitized K_D , μ M	Open IC_{50} , μ M		
			41 \pm 9 (2 2; Rat)	-50	
			60 \pm 18 (3 2; Rat)	-50	
			0.81 (nicotine-elicited hippocampal noradrenaline release; Rat)	0	[119]
Lidocaine	>1000 (<i>T. ocellata</i>)	150 \pm 10 (<i>T. ocellata</i>)		0	[114]
Piperocaine	0.33 \pm 0.08 (<i>T. ocellata</i>)	4.2 \pm 1.1 (<i>T. ocellata</i>)		0	[114]
	0.8 (<i>T. californica</i>)	55 (<i>T. californica</i>)		0	[70]
Benzocaine			114 \pm 48 (<i>Rana temporaria</i> muscle)	-70	[120]
	500 \pm 50 (<i>D. tschudii</i>)			0	[69]
Dibucaine	3.0 (<i>T. californica</i>)	0.24 (<i>T. californica</i>)		0	[121]
Bupivacaine	25 \pm 5 (<i>T. californica</i>) 32 \pm 3	3 \pm 1 (<i>T. californica</i>) 6 \pm 1		0 0	[58]
Bupivacaine Methiodide	3.2 \pm 0.4 (1 2 1 ; Rat) 1.8 \pm 0.4	0.75 \pm 0.08 (1 2 1 ; Rat) 0.56 \pm 0.06		0 0	[58]
QX-222			29 (Frog muscle)	-120	[47]
			28 (Parasympathetic neurons)	-80	[4]
			20 (Rat myoballs)	-120	[60]
			141 (4 2; Mouse) 18 (1 2 1 ; BC ₃ H-1)	-150 -150	[48]
			76.5 \pm 7.8 (1 2 1 ; Mouse) 20.0 \pm 0.9 (1 2 1 ; Mouse)	-110 -150	[52]
			9 (<i>Rana pipiens</i> muscle)	-80	[61]
QX-314			1 (Frog muscle)	-100	[47]
C6SL-MeI	20 (<i>T. californica</i>)	0.87 (<i>T. californica</i>)		0	[122]
Group II					
Proadifen	7 (<i>T. californica</i>)	0.6 (<i>T. californica</i>)		0	[123]
Meproadifen	6.2 \pm 3.0 (<i>T. marmorata</i>)	0.5 \pm 0.2 (<i>T. marmorata</i>)		0	[67]
	25 (<i>T. californica</i>)	0.3 (<i>T. californica</i>)		0	[123]
Adiphenine	5 \pm 2 (<i>T. californica</i>)	7 (<i>T. californica</i>)		0	[124]
Group III					
Dimethisoquin	5.0 (<i>T. californica</i>)	1.1 (<i>T. californica</i>)		0	[121]
Trimethisoquin	3.2 \pm 0.9 (<i>T. marmorata</i>)	1.2 \pm 0.3 (<i>T. marmorata</i>)		0	[67]

Binding experiments with [³H]trimethisoquin demonstrated that the low-affinity site concentration increases whereas the high-affinity site concentration remains without change when the lipid content of AChR reconstituted systems is augmented, suggesting a lipid-protein localization for low-affinity LA binding sites [67]. More recently, photoaffinity labeling data indicate that [³H]tetracaine is incorporated in a fragment containing the 1M4 transmembrane domain [70]. These results support the conjecture that low-affinity binding sites are in fact located at the lipid-protein interface. Within this scenario, it is reasonable to think that the lipid-protein interface of the AChR may also be the target site for hydrophobic spin-labeled LAs (LASLs). To this end, the interaction of different LASLs with the lipid-protein interface of the AChR was studied by means of electron paramagnetic resonance (EPR) spectroscopy [71] (reviewed in [3, 7, 29]). By analogy with the dynamics of lipid molecules at the lipid-protein interface, it is feasible that LA motion becomes

slower when the molecule interacts with the protein. Thus, the signal provided by LASLs at the lipid-protein interface is distinguishable from the signal in the bulk lipid membrane. In practice, both signals can be separated by spectral subtraction. This consists of subtracting the signal provided by LASL molecules in a membrane suspension of previously extracted lipids (the membrane mobile component) of the tissue or cell under study from the total signal (both protein-perturbed and membrane-mobile components) of the same spin-label in protein-containing native or reconstituted membranes. In this regard, different laboratories have used either AChR-rich membranes or AChR-dioleoylphosphatidylcholine (DOPC) reconstituted system, and liposomes furnished with either electric organ-extracted total lipids or pure DOPC.

The data shown in Table 3 indicate that there is an appreciable fraction (*f*) of LASL molecules interacting with the lipid-protein interface of the AChR. However, depending

Table 3. Relative Affinity of Spin-labeled Local Anesthetic Analogs for the Lipid-protein Interface of the *Torpedo* AChR

Affinity	Experimental Conditions	Spin-labeled Local Anesthetic Analogs ^a	<i>f</i> ^b	K_a^{LASL}/K_a^{PCSLc}	G_{LASL}^d kJ/mol	References
High	Reconstituted DOPC:AChR 150:1 molar ratio	C6SL	0.77	-	-	[72]
	Reconstituted DOPC:AChR 97:1 molar ratio	C6SL-MeI	0.67	-	-	[73]
	Native membranes pH 6.0	C6SL	0.60	-	-	[72]
	Reconstituted DOPC:AChR 209:1 molar ratio	C6SL-MeI	0.52	-	-	[73]
	Native membranes pH 7.4	IX	0.36	2.4	-2.1	[71]
		Benzocaine-SL (I)	0.35	2.3	-2.0	
		Thioprocaine-SL (III)	0.34	2.2	-1.9	
Intermediate	Native membranes pH 7.4	V	0.31	1.9	-1.6	
		VI ⁺ /Me	0.31	1.9	-1.6	
		X	0.31	1.9	-1.6	
		IV	0.29	1.7	-1.4	
		VIII	0.28	1.7	-1.2	
		VI	0.27	1.6	-1.1	
Low	Native membranes pH 7.4	Procaine-SL (II)	0.23	1.3	-0.6	
	Reconstituted DOPC:AChR 284:1 molar ratio	C6SL-MeI	0.23	-	-	[73]
	Reconstituted DOPC:AChR 560:1 molar ratio	C6SL	0.14	-	-	[72]

^a The molecular structure of LASLs are shown in Fig. (3).

^b The protein perturbed component for each LASL was obtained by means of spectral subtractions [71].

^c The relative association constant for each LASL was obtained according to Eq. (1) with respect to 14-PCSL ($f_{PCSL} = 0.19$; [71]), a lipid with known low specificity for the lipid-protein interface (reviewed in [3, 7, 29]).

^d The relative association free energy change of each LASL was calculated according to Eq. (2).

on which AChR membrane preparation are studied, the temperature and pH at which the EPR measurement was performed, or the lipid:protein molar ratio of the reconstituted system, a broad range of f values is obtained. For reconstituted membranes, the f values for the methyl-doxyamine intracaine derivative (C6SL) depend on the lipid:protein ratio [72]. For example, the f value changed from 0.77 to 0.14 when DOPC:AChR molar ratios of about 150:1 to 560:1 were respectively studied. The same basic result was obtained using the quaternary derivative C6SL-MeI [73]. For experiments with native membranes, we compared the f value of each LASL with the value obtained for 14-doxyphosphatidylcholine (14-PCSL; $f_{\text{PCSL}} = 0.19$), a lipid with known low affinity for the hydrophobic surface of the AChR (reviewed in [3, 7, 29]). In this regard, the association constant for each LASL relative to PCSL ($K_a^{\text{LASL}}/K_a^{\text{PCSL}}$) was calculated according to the equation:

$$K_a^{\text{LASL}}/K_a^{\text{PCSL}} = [(1 - f_{\text{PCSL}})/f_{\text{PCSL}}] / [(1 - f)/f] \quad (1)$$

The calculated values were summarized in Table 3. The relative constant values allow us to discriminate among LAs interacting with high, intermediate, and low specificity with the AChR.

Concomitantly, the energy related to the selectivity of the LASL-protein interaction can be obtained relative to PCSL. For this purpose, the differential energy of association of each LASL with respect to 14-PCSL (G_{LASL}) was calculated using the expression:

$$G_{\text{LASL}} = -RT \ln(K_a^{\text{LASL}}/K_a^{\text{PCSL}}) \quad (2)$$

where R is the universal gas constant and T is the absolute temperature used in the EPR experiment. The calculated values were also included in Table 3.

Fluorescence-quenching is another spectroscopic method that has been successfully used to measure the efficiency of different LASLs to quench the intrinsic fluorescence of the AChR protein [71], and to determine the effect of several LAs on the interaction of the cholesterol analogue doxyl-cholestane (CSL) with the lipid-protein interface [74]. The protein intrinsic fluorescence originates from Trp and Tyr residues. Of the 51 Trp residues on the *Torpedo* AChR, only one is found in the transmembrane domain, specifically Trp⁴⁵³ in the M4 domain of the subunit. It has been hypothesized that because of the location of Trp⁴⁵³ in a hydrophobic environment, the quantum yield of this residue is higher than that for the other Trp groups, producing 30% of the total AChR intrinsic fluorescence intensity. However, direct fluorescence measurements of M4 peptides dissolved in detergent indicate a lower intensity than previously considered (H.R. Arias and M.P. Blanton, unpublished results).

The Trp⁴⁵³ transverse distance from the inner lipid membrane surface (from the phospholipid headgroup region) was measured by the parallax method and was found to be 10 Å [75]. Thus, hydrophobic quenchers such as LASLs and CSL may interact with this residue from the lipid phase. In fact, both Benzocaine-SL (I) and Thioprocaine-SL (III) [71] as well as CSL [74] were found to efficiently quench

the AChR intrinsic fluorescence. Since fluorescence-quenching is a short range process (within a distance of 5 Å between the van der Waals radii), higher quenching efficiency indicates more accessibility of the quencher to the domain where the fluorophore is attached. For this purpose, the quenching parameters were graphically calculated by plotting I_0/I versus $1/[Q]$ according to the modified Stern-Volmer equation (reviewed in [3, 7, 29]):

$$I_0/I = 1/(f_a K_Q [Q]) + 1/f_a \quad (3)$$

where I is the difference between the intensities of the intrinsic AChR fluorescence in the absence (I_0) or in the presence (I) of different concentrations of the quencher $[Q]$. K_Q is the apparent steady-state Stern-Volmer quenching constant, and f_a is the apparent fraction of available fluorophores. The calculated quenching parameters for LASLs are summarized in Table 4. Alternatively, the same parameters can be obtained from the plot τ_0/τ versus $1/[Q]$, according to the equation:

$$\tau_0/\tau = 1/(f_a K_Q' [Q]) + 1/f_a \quad (4)$$

where τ is the difference between the lifetimes of a certain fluorophore attached to the AChR in the absence (τ_0) or in the presence (τ) of different concentrations of the quencher $[Q]$, and K_Q' is the apparent lifetime Stern-Volmer quenching constant, which in turn is equal to k_q/k_{q_0} , where k_q is the bimolecular quenching rate constant [76].

Comparing the f_a values it is possible to deduce that Benzocaine-SL is accessible to a higher fraction of Trp groups than procaine thioester spin-label. This is in accord with the putative position of benzocaine binding site(s) at the aqueous-lipid-protein interface [68], where a higher amount of Trp residues, including the ones from the extracellular portion of the AChR (up to 50 Trps), can be quenched. In this regard, quenching experiments designed to demonstrate that LAs effectively displace the binding of CSL at the lipid-AChR interface [74] support this assumption. More specifically, the quenching parameters shown in Table 5 indicate that benzocaine diminishes by 11-fold the quenching efficiency of CSL suggesting that the benzocaine binding sites partially or totally overlap with those for cholesterol. If we consider that the binding sites for cholesterol are located at the nonannular lipid domain [30] (reviewed in [3, 7, 29]), then, benzocaine binding sites should be close to this lipid domain. However, Addona *et al.* [77] found no appreciable difference on agonist-induced activation of AChRs reconstituted in phosphatidylcholine, phosphatidic acid, and either cholesterol hemisuccinate covalently attached to the glycerol backbone of phosphatidylcholine (which will be restricted to the annular lipid domain) or cholesterol (presumably located at the nonannular lipid domain), and coined the term periannular to define the location of cholesterol binding sites as very close to the lipid-protein interface. These results are in agreement with photoaffinity labeling experiments using [¹²⁵I]azido-cholesterol [78]. [¹²⁵I]Azido-cholesterol was incorporated in fragments containing the M1 and the M4 transmembrane domain, suggesting that cholesterol binding sites are localized at the lipid-protein interface. Thus, considering the possibility that cholesterol binding sites are located closer to

Table 4. Quenching Efficiency of Local Anesthetic Analogs on Intrinsic and Extrinsic AChR-attached Fluorophore Fluorescence

Local Anesthetic Analog	AChR Conformational State	f_a^c	K_Q^d mM^{-1}	$1/K_Q^f$ μM	References
AChR-attached Trp residues^a					
Thioprocaine-SL	Resting	0.40	180	6	[71]
	Initially Activated	0.51	50	20	
	Desensitized	0.44	110	9	
Benzocaine-SL	Resting	0.67	33	30	
	Initially Activated	0.99	18	56	
	Desensitized	0.65	45	22	
AChR-labeled pyrene^b					
			K_Q^e mM^{-1}	$1/K_Q^f$ μM	
Tetracaine	Resting	-	0.57 ± 0.01	1754	[81]
	Resting (-BTx)	-	0.61 ± 0.01	1639	
	Desensitized	-	0.60 ± 0.05	1667	

^a Considering that each quenching titration was performed in the absence of CCh, or alternatively was co-incubated or preincubated with 100 μM CCh, the AChR should be in the resting, initially activated, or desensitized state, respectively.

^b The lifetime of AChR-labeled pyrene was determined in the absence of agonist (resting state), in the presence of 0.25 μM -BTx (resting state), or in the presence of 1 mM CCh (desensitized state), respectively.

^c The apparent fraction of available fluorophores in the protein was determined from the y-intercept of the modified Stern-Volmer plot, $f_a = 1/\text{y-intercept}$, according to Eq. (3).

^d The apparent steady-state Stern-Volmer constant was calculated from the y-intercept/slope ratio of the modified Stern-Volmer plot according to Eq. (3).

^e The apparent lifetime Stern-Volmer constant was calculated from the data of González-Ros *et al.* [81], according to Eq. (4).

^f Relative concentration of the LA analog at which 50% of the fluorescence intensity (or lifetime) is quenched assuming that the AChR-attached fluorophore is totally available to LA quencher ($f_a = 1$).

the annular lipid domain, benzocaine might also bind to this lipid domain.

Table 5. Local Anesthetic Inhibition of Doxyl-cholestane Quenching Efficiency on the AChR Intrinsic Fluorescence

Local Anesthetic	f_a^a	K_Q^c mM^{-1}	$1/K_Q^d$ μM
None	0.45	204	4.9
30 μM QX-222	0.38	65	15.4
30 μM Tetracaine	0.31	51	19.8
30 μM Benzocaine	0.99	18	56.3
3 μM Procaine	0.99	26	38.0

^{a, b, c} Same as the legend from Table 4. The observed values were obtained according to Eq. (3) [74].

In addition to benzocaine, other LAs diminish the quenching efficiency of CSL with potencies that are in the sequence: procaine > benzocaine > tetracaine > QX-222 (Table 5) [74]. There are two possible explanations for the observed variance among LAs: distinct membrane solubility

for each LA or a slightly different location for each LA binding site. The first possibility is unlikely since the calculated apparent partition coefficient for benzocaine ($5,800 \pm 1,000$), procaine ($1,700 \pm 800$) (H.R. Arias, unpublished results), and tetracaine ($2,200 \pm 600$; [79]) in AChR native membranes do not follow the same sequence pattern. Thus, the idea that each specific LA binds to partially overlapping nonannular (or periannular) sites seems to be more likely. However, procaine, the LA that most potently inhibited the CSL-AChR interaction, does not perturb quinacrine binding to the nonannular lipid domain (H.R. Arias, unpublished results). This result is in agreement with a peri-annular location for LAs, or at least for procaine.

The fact that Thioprocaine-SL shows a higher efficiency than Benzocaine-SL to quench a lower fraction of available AChR fluorophores suggests that the former analog is sensing the transmembrane M4Trp⁴⁵³ residue. Thus, considering that Trp⁴⁵³ is located at the nonannular lipid domain (reviewed in [3, 7, 29]), the thioprocaine binding site(s) would be closer to this particular lipid domain. However, photoaffinity labeling experiments demonstrate that the uncharged compound 2-[³H]diazofluorene non-specifically photoincorporates into Trp⁴⁵³, suggesting that this residue is located at the lipid-protein interface [80]. In

this regard, the binding sites for thioprocaine may be closer to the annular lipid domain.

In addition, to use the intrinsic fluorescence, the employment of extrinsic fluorophores might help to specify the binding site location for LAs. In this regard, measuring the tetracaine quenching efficiency on AChR-labeled pyrene lifetime fluorescence, an effective accessibility of tetracaine to this particular site was suggested [81]. Unfortunately, the exact site where pyrene-1-sulfonylazide labels the AChR has not been determined as yet. Nevertheless, the evidence indicating that both Benzocaine-SL and Thioprocaine-SL seem to be 60-300 times more accessible to the Trp domain than tetracaine is accessible to the pyrene-attached site (Table 3), suggests that pyrene is attached at a domain far from the M4Trp⁴⁵³ residue. A potential residue might be Cy⁴¹² from the 1 subunit, which is located at the edge of the lipid-exposed helical face. To determine the exact location of low-affinity LA binding sites at the lipid-protein interface further experiments need to be performed.

Another way to obtain structural information from the AChR is by studying the effect of LAs on the AChR conformational state. In this regard, the elicited agonist effect on AChR-LA interactions is shown in Table 4. For example, the differences in the concentration at which 50% of the initial intensity is quenched ($1/K_Q$), considering that all fluorophores are fully accessible to the quencher, indicate that a higher concentration of both Benzocaine-SL and Thioprocaine-SL is necessary to quench a greater fraction of AChR-attached Trp residues when the receptor is initially activated (coincubation) by carbamylcholine (CCh) than

when the AChR is either in the resting (no CCh) or in the desensitized (preincubated) state (Table 4). This may be explained by considering that the receptor protein changes its conformational state upon agonist activation and after a relatively long span (seconds to minutes), this structural change may be sensed by the LA over quite considerable distances to the lipid-protein interface. On the contrary, the quenching efficiency of both LASLs do not change significantly when the AChR converts from the resting to desensitized form. In addition, different cholinergic ligands do not change the quenching efficiency of unlabeled tetracaine on AChR-labeled pyrene fluorescence [81] (see Table 4). This indicates that the ligand-induced AChR conformational changes are not sensed at the pyrene-attached domain.

EPR studies on the effect of agonist on the interaction of several LASLs with the AChR also produce interesting results. Several LASL derivatives displayed a slightly lower affinity for the AChR in the presence of CCh (Table 6). The same basic results were obtained when AChR-containing membranes were preincubated with C6SL (or alternatively with C6SL-MeI) and then incubated with CCh or when both ligands were incubated together. In this latter procedure, a fraction of AChRs may be initially activated by CCh. Interestingly, the f value for the quaternary C6SL-MeI derivative diminished 10-fold. Contrary to the evidence observed on tertiary LASLs, the binding of C6SL-MeI to the desensitized AChR was inhibited by 80-90% (Table 6). The obtained results are in agreement with the hypothesis that both charged and uncharged LAs reach its binding site(s) during the initial step of agonist stimulation, but when the

Table 6. Agonist-elicited Modulation of Spin-labeled Local Anesthetic Binding to the AChR

Spin-Labeled Local Anesthetic Analog ^a	Agonist	AChR Conformational State	f ^b	Binding (%)	References
Thioprocaine-SL (III)	None	Resting	0.35	100	[71]
	CCh	Desensitized	0.34	97	
Benzocaine-SL (I)	None	Resting	0.32	100	
	CCh	Desensitized	0.31	97	
Procaine-SL (II)	None	Resting	0.25	100	
	CCh	Desensitized	0.22	88	
C6SL	CCh (post- or coincubation with C6SL)	Initially Activated or Desensitized	-	100	[122, 125]
	CCh (preincubation)	Desensitized	-	100	
C6SL-MeI	CCh (post- or coincubation with C6SL-MeI)	Initially Activated or Desensitized	-	100	
	CCh (preincubation)	Desensitized	-	10-20	
	CCh (coincubation)	Desensitized	0.48 (1:1) ^c	-	
			0.30 (3:1) ^c	-	
			0.20 (10:1) ^c	-	

^a See molecular structures in Fig. (4).

^b The fraction of protein perturbed component was obtained by spectral subtraction [71].

^c Values in parenthesis correspond to C6SL-MeI:AChR molar ratios.

Table 7. Stoichiometry of High-affinity Local Anesthetic Binding Sites on the AChR

Local Anesthetic	Binding site(s) per AChR	Methodology	Reference
Meproadifen	0.5 ± 0.1	[³ H]Meproadifen equilibrium binding	[82]
	0.6 ± 0.2	[¹⁴ C]Meproadifen equilibrium binding	[83]
Trimethisoquin	0.75	5-Azido [³ H]trimethisoquin photolabeling	[85]
	0.5-0.6	5-Azido [³ H]trimethisoquin photolabeling	[86]
	1.5 ± 0.1	[³ H]Trimethisoquin equilibrium binding	[84]
Tetracaine	0.86 ± 0.14	[³ H]Tetracaine equilibrium binding	[70]

AChR becomes desensitized and in turn, the channel is closed, the equilibrium binding of LA molecules is prevented. However, tertiary LAs may reach their binding site in the AChR desensitized (closed) state, supporting the existence of a regulatory LA site which is occupied even when the ion channel is closed.

HIGH-AFFINITY LOCAL ANESTHETIC BINDING SITES

In addition to low-affinity LA binding sites, there exist high-affinity LA binding sites (each one for a specific LA) which are displaced by HTX or other high-affinity NCIs. Thus, these LAs form part of the group of high-affinity NCIs. The evidence that high-affinity LAs present a stoichiometry of one binding site per functional AChR was determined by equilibrium binding of radiolabeled LAs such as meproadifen [82, 83] and trimethisoquin [84] as well as by 5-azido trimethisoquin photolabeling [85, 86] (Table 7). More recently, the stoichiometry of [³H]tetracaine binding was determined in the AChR resting state [70]. Averaging all the experimental values showed in Table 7, a stoichiometric ratio of 0.79 ± 0.37 LA binding site per AChR is calculated. This ratio, which is close to unity, is similar to other high-affinity NCIs (reviewed in [29]).

Local anesthetics discriminate among different AChR conformational states [R, O, and D; see Fig. (2)]. For instance, the decrease in the K_{dS} in the presence of agonists,

as showed in Table 2, is consistent with the preferential binding of LAs (from Group II and III and some from Group I), as well as other NCIs, to the desensitized AChR. However, some LAs from Group I (e.g., procaine) do not have any preference with respect to the resting or the desensitized AChR, whereas others [e.g., tetracaine and piperocaine (see Table 2)] prefer the AChR in the resting state. In addition, some LAs from Group I (e.g., QX-222) bind better the AChR in the open conformational state.

Interestingly, the affinity of LAs for muscle AChRs seems to be different to that from neuronal AChRs, and they also discriminate between distinct neuronal-type AChRs (Table 2). In particular, procaine has a lower K_d for the receptor found in parasympathetic neurons [4] than that for the other receptors. On the contrary, QX-222 binds the α_2 receptor with affinities one order of magnitude lower than other AChRs at the same voltage membrane (e.g., -90 mV; [48]). In addition, (-)cocaine has a lower IC_{50} value for the α_4 receptor than for other neuronal-type AChRs [49]. The observed differences in affinities (Table 2) conjointly with the distinctions in voltage sensitivity (Table 1) existent among LAs on several AChRs might help to identify the structural components involved in the LA binding site.

One of the most important techniques used to discern the localization of high-affinity LA binding sites is the photoaffinity labeling approach. This can be achieved using radiolabeled LAs that can be directly activated by UV light, or using other photoactivatable derivatives with specific

Table 8. Photolabeling of the AChR by Local Anesthetic Analogs

Local Anesthetic Analog	Subunit	Domain	Ring	Residues	References
Azido [³ H]procainamide	1				[126]
5-Azido [³ H]trimethisoquin					[86]
[³ H]Trimethisoquin					[67, 87]
[³ H]Meproadifen mustard	1	Close to the M2 portion of the M2-M3 loop	Outer or Extracellular	Glu ²⁶²	[88]
[³ H]Tetracaine	1 1	M2	Leucine Valine Position 5 Position 12	1Leu ²⁵¹ , 1Leu ²⁵⁷ , Leu ²⁶⁰ , and Leu ²⁶⁵ 1Val ²⁵⁵ and Val ²⁶⁹ 1Ile ²⁴⁷ Ala ²⁶⁸	[70, 95]

photoreactive groups. Table 8 summarizes the information on LA binding site location using different LA probes. The specificity of the photoaffinity labeling experiments followed the criteria: (a) existence of a positive displacement elicited by other known NCIs such as HTX or PCP, (b) enhancement of affinity and thus labeling of the LA under study (but not for all) in the presence of agonists, and (c) inhibition of the agonist effect by competitive antagonists such as α -BTx.

One of the first labeling experiments to localize the LA binding site was performed using different azido LA derivatives (reviewed in [3]). The azido-procainamide derivative only labeled the AChR α subunit, whereas the 5-azido[3 H]trimethisoquin derivative labeled the β subunit in a HTX- and CCh-sensitive fashion (Table 8). The same basic pattern was observed using [3 H]trimethisoquin and simple

UV irradiation [67, 87]. Similar results were observed using other tritiated NCIs (reviewed in [29]). The LA analog meproadifen mustard, as well as other NCIs, also labeled the α and β subunit [88].

Binding Sites for Quaternary Local Anesthetics

The outer or extracellular ring is the labeling site for the potent LA derivative meproadifen mustard. Meproadifen mustard was initially found in a fragment beginning at Ser¹⁷³ of the α subunit. More precisely, the meproadifen derivative labeled the α subunit at position Glu²⁶² [88] (Table 8). Based on the four transmembrane AChR structural model [see Fig. (1)], there is consensus that this ring of negative charges is located between the synaptic membrane and the extracellular domain of the AChR (the M2-M3 loop,

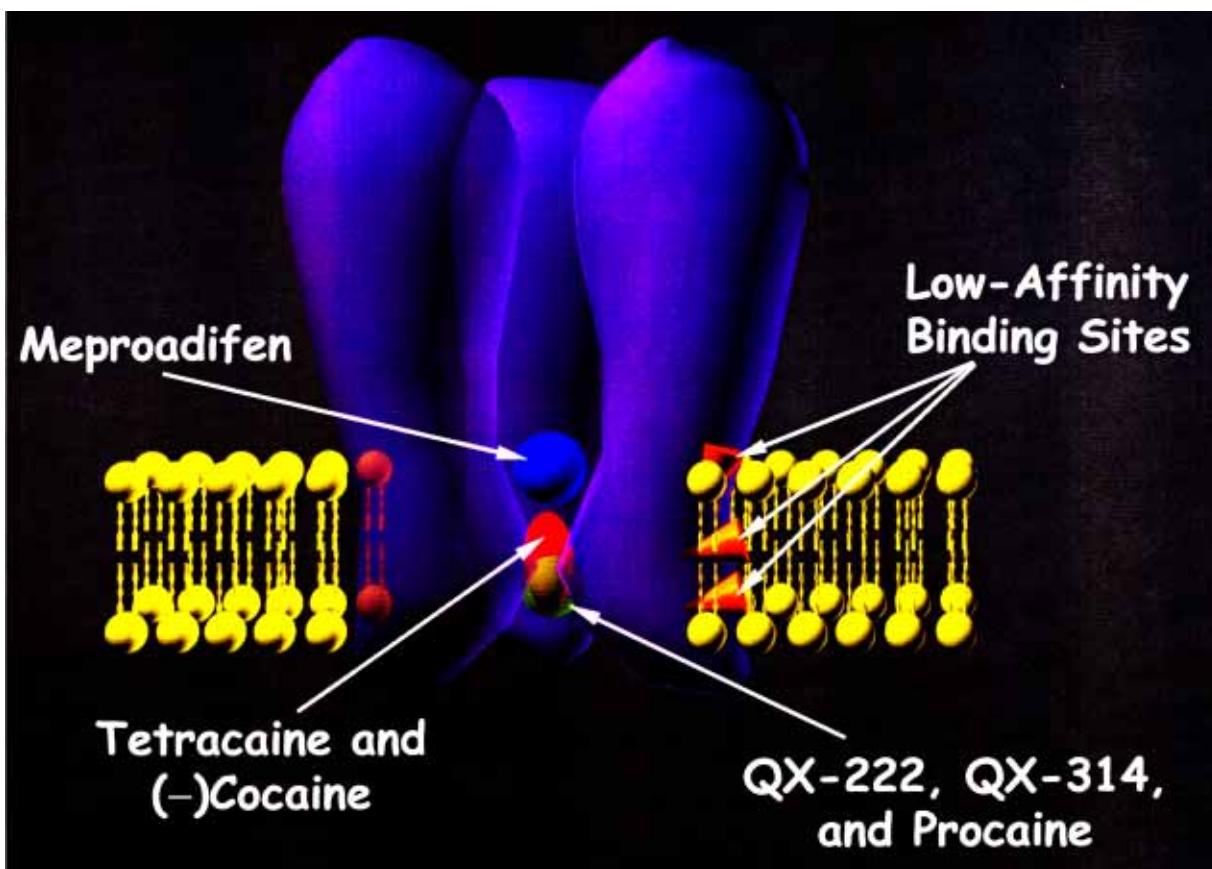


Fig. (6). Transverse schematic view of the AChR (only three subunits are shown for simplicity) showing the most probable localization for several local anesthetic binding sites. The photolabeling site for meproadifen mustard (blue) is located at the extracellular or outer ring of the desensitized AChR. Additional photoaffinity labeling studies indicate that the binding site for tetracaine (red) is located between the serine and the valine ring (including the leucine ring) of the resting AChR. Mutagenesis experiments and accessibility studies indicate that the locus for QX-222 and QX-314 as well as for procaine (green) is positioned at both the serine and the leucine ring in the open ion channel conformation. Additional mutagenesis studies in the open state suggest that the (-)cocaine binding site (red) is located at the valine ring and perhaps at the serine ring. The orange cones indicate the possible location of low-affinity sites for local anesthetics such as benzocaine, procaine, tetracaine, and QX-222. Among them, there is an increasing amount of data indicating that benzocaine molecules bind to the aqueous-lipid-protein interface.

closer to M2), probably at or near the internal mouth of the channel [Fig. (6)]. Interestingly, using a photoactivatable alcohol derivative, 3-[³H]azidoctanol, which acts as a general anesthetic in tadpoles, potentiates GABA_AR activity, and inhibits *Torpedo* AChRs [89], the same residue (Glu²⁶²) was labeled [90]. These results indicate that the LA meproadifen (and probably its tertiary analog proadifen) shares the same binding locus as general anesthetic alcohols.

Meproadifen, as well as other LAs, shifts the equilibrium to the desensitized state (see Table 2). This was evidenced when the labeling of ¹Tyr⁹³, an amino acid involved in the agonist/competitive antagonist binding site at the ¹ subunit (reviewed in [6]), elicited by the irreversible antagonist *p*-N,N-(dimethylamino)phenyldiazonium fluoroborate was augmented in the presence of meproadifen. This experimental evidence suggests that this residue is more accessible to labeling when the AChR is in the desensitized state.

The side chains of photolabeled amino acids such as ¹Ser²⁴⁸ for the neuroleptic and NCI chlorpromazine (CPZ)

and ¹Glu²⁶² for the LA meproadifen should be approximately 15 Å apart from each other. This fact provides support for the extension of the early hypothesis of only one locus for structurally-unrelated high-affinity NCIs to the existence of several binding sites for different NCIs all located into the channel lumen (reviewed in [3, 29]).

The localization of the QX-222 binding site was proposed on the basis of site-directed mutagenesis and patch-clamp studies [52, 53] (reviewed in [3, 6, 29]). For instance, the pharmacological activity of the open-channel blocker QX-222 is affected when the serine ring (position 6) is mutated (see Table 9). The drug presented shorter time in the AChR-bound state and its K_d was augmented when the polar amino acid ¹Ser²⁴⁸ was mutated to Ala, a nonpolar amino acid. In comparison, the Ser²⁶²Ala mutation also affected these properties but in an extent two times lower than the one detected in the ¹ subunit. This effect can be interpreted in the light of difference in the number of residues mutated (there are two ¹ subunits per each). A double mutation (actually a triple mutation) produced an additive effect on the K_d of QX-222. However, the observed lifetime (1.5 ms) for

Table 9. Residue Mutations on the M2 Transmembrane Domain of Different AChRs Affecting Local Anesthetic Affinity

Local Anesthetic	Mutation	Source of AChR	Pharmacological effect (fold)		References
			Affinity Increase	Affinity Decrease	
QX-222	¹ Ser ²⁵² Ala	Mouse ¹ ₂ ¹	1.9	-	[52]
	¹ Thr ²⁶³ Ala		1.8	-	
	¹ Ser ²⁵² Ala/ ¹ Thr ²⁶⁵ Ala		3.4	-	
	¹ Ser ²⁴⁸ Ala		-	2.0	
	¹ Phe ²⁵⁹ Ser		1.7	-	
	Ser ²⁶² Ala		-	1.3	
	¹ Ser ²⁴⁸ Ala/ Ser ²⁶² Ala		-	2.7	
	¹ Thr ²⁴⁴ Ala		1.2	-	
	¹ Gly ²⁵⁵ Ser		1.3	-	
	Thr ²⁵³ Ala		1.3	-	
	Ser ²⁵⁸ Ala		-	1.1	
	¹ Thr ²⁴⁴ Ala/ ¹ Gly ²⁵⁵ Ser		-	1.3	
	Thr ²⁵³ Ala/ Ser ²⁵⁸ Ala		-	1.5	
	¹ Ser ²⁵² Ala	Mouse ¹ ₂ ¹ ² (-less)	1.4	-	[48]
	¹ Phe ²⁵⁹ Ser		1.3	-	
	Thr ²⁶⁴ Pro	Mouse ¹ ₂ ¹	1.5	-	[88]
	⁷ Leu ²⁴⁷ Thr (or Ser)	Chick ⁷	-	Abolished	[92]
⁷ Leu ²⁴⁷ Phe		-	1.5		
⁷ Leu ²⁴⁷ Val		-	1.1		
Procaine	¹ Ser ²⁵² Ala/ ¹ Thr ²⁶⁵ Ala	Mouse ¹ ₂ ¹	3.0	-	[99]
(-)Cocaine	⁴ Phe ²⁵⁵ Val	Rat ³ ⁴	-	8.3	[49]
	² Val ²⁵³ Phe	Rat ³ ²	3.5	-	

QX-222 in the wild type AChR is similar (1.2 ms) to that obtained in the double mutated [52]. Additional mutations on position 2 (see Table 9) produce a similar pattern as that observed by mutations on position 6, however, the effect on the QX-222 K_d was small. In contrast with the experimental evidence on serine ring mutations, when 1Ser²⁵² (position 10: located one residue apart from the leucine ring) was mutated to Ala, both the affinity of QX-222 and the lifetime of the AChR-QX-222 complex were enhanced. The increased affinity was principally due to a decrease in the dissociation rate constant values and it was not affected by voltage membrane changes [52]. Mutations 1Phe²⁵⁹Ser and 1Ser²⁵²Ala on the $\alpha_1\beta_1\gamma_2$ (-less) receptor showed similar relative effect of QX-222 blockade as in the $\alpha_1\beta_1$ receptor [51]. The Thr²⁶⁴Pro mutation in the β_1 subunit, which has been implicated as responsible of one of the congenital myasthenic syndromes (reviewed in [3]), only slightly affects the inhibitory property of QX-222 [91] (Table 8). Thus, Thr²⁶⁴, which is located close to the valine ring, may not be involved in the QX-222 binding site. In addition, QX-222 produced the same effect on both adult ($\alpha_1\beta_1$) and embryonic ($\alpha_1\beta_1$) muscle-type AChRs (see Table 2). Considering that the structural determinants that account for the functional differences between both channels are located at the M3-M4 loop, the M4 segment, and the extracellular portion of both channels (reviewed in [3]), the QX-222 locus should be positioned neither in the extracellular nor cytoplasmic hydrophilic portions nor in the M4 transmembrane fragment but, as was previously addressed, within the ion channel.

Concerning neuronal AChRs, QX-222 has been shown to block the AChR in rat parasympathetic ganglion cells, in the clonal cell line PC12, in the α_7 subtype, and in the $\alpha_4\beta_2$ neuronal receptor (see Table 2). Notably, the $\alpha_4\beta_2$ receptor type showed a much lower sensitivity to QX-222 than other AChRs. The structural components that confer this affinity distinctions might be elucidated by considering which amino acids on the M2 domain of the AChR types are different. In chick brain α_7 receptors, the pharmacological effect of QX-222 was abolished by mutation of the leucine ring, in particular Leu²⁴⁷ to polar residues such as Thr or Ser [92] (Table 9). As expected, mutations on amino acids related to the agonist binding site on the α_7 AChR, did not significantly change the pharmacological properties of QX-222 (reviewed in [3]).

Based on these results, it is conceivable that the quaternary ammonium group of QX-222 is positioned close to Ser²⁴⁸, which is part of the conserved serine ring (position 6). Taking into account that the secondary structure of the M2 transmembrane domain of the α_1 subunit is α -helical, Ser²⁴⁸ would be positioned one turn away from Ser²⁵². In turn, 1Ser²⁵² (position 10) is located one residue apart from the leucine ring (position 9). Thus, the aromatic moiety of the QX-222 molecule is near the leucine ring, 5.7 Å away from the serine ring (reviewed in [3, 7, 29]). Interestingly, based on the susceptible residues affecting binding affinity and using molecular modelling, the QX-222 molecule was fitted into the channel lumen [93].

The blocking rate of QX-314 is similar to that of its triethylamine structural analog QX-222. However, QX-314

remains in the ion channel for longer time (an order of magnitude more) than QX-222 does. Thus, QX-222 is termed a fast channel blocker whereas QX-314 is called a slow channel blocker. Nevertheless, testing the protection elicited by QX-314 on the reaction of methanethiosulfonate derivatives with several Cys-substituted (one at a time) residues in the M2 segment of the mouse α_1 subunit, Pascual and Karlin [94] considered that both LAs practically share the same locus. When the channel was open, QX-314 protects completely the Cys mutants on the α_1 subunit located at Glu²⁴¹, Thr²⁴⁴, and Ser²⁴⁸, and moderately those located at Leu²⁵¹ and Val²⁵⁵, whereas both Leu²⁵⁸ and Glu²⁶² to Cys mutants were not protected by the drug. This evidence suggests that QX-314 binds to the open ion channel and that its locus is found at residues located between Glu²⁴¹ and Leu²⁵¹ of the 1M2 domain. The portion of the channel containing the sequence between Gly²⁴⁰ and Thr²⁴⁴ is close to the cytoplasmic side of the ion channel and it is suggested to be involved in the activation gate [34]. In addition, no protection was observed when the channel was in the resting [94] or in the desensitized [36] state. Another possibility is that QX-314 binds to the same site as QX-222 [see Fig. (6)] at the portion between 1Ser²⁴⁸ and 1Ser²⁵², and thus, the passage of the methanethiosulfonate reagent to the Cys-substituted residues located in a more constricted region of the ion channel, namely the gate, is consequently inhibited.

Binding Sites for Tertiary Local Anesthetics

Previous experiments demonstrate that specific labeling of the NCI 3-(trifluoromethyl)-3-*m*-([¹²⁵I]iodophenyl) diazine ([¹²⁵I]TID) of the AChR is inhibited by tetracaine and dibucaine in the presence of -BTx (reviewed in [3]). This is in accord with the fact that tetracaine binds preferentially the AChR in the resting state (see Table 2). Thus, tetracaine might be competing with [¹²⁵I]TID labeling by a mutually exclusive mechanism. Since the TID binding site has been found to be located at the valine and leucine rings (reviewed in [29]), the tetracaine locus should be close to these rings. In fact, photoaffinity labeling studies using [³H]tetracaine under UV activation indicate that this LA incorporates with similar efficiency to α_1 , α_2 , and α_3 subunits [70]. More specifically, [³H]tetracaine labeled two sets of homologous hydrophobic residues: one comprised of 1Leu²⁵¹, 1Leu²⁵⁷, Leu²⁶⁰, and Leu²⁶⁵ [leucine ring (position 9)] and another formed by 1Val²⁵⁵ and Val²⁶⁹ [valine ring (position 13)] as well as residues Ala²⁶⁸ (position 12) and Ile²⁴⁷ (position 5) [95] (see Table 8). The residues from both subunits are almost coincident with the TID-labeled amino acids in the resting state as well as with the CPZ-labeled amino acids in the desensitized state (valine and leucine rings). In this regard, a model for the tetracaine binding site was suggested [95]. Figure (7; Top) depicts the basic details of this model: the benzene ring (6.5 Å) is positioned at the leucine ring (position 9) with its *N*-butyl chain (4 Å wide in extended configuration) interacting with hydrophobic residues from both position 12 and 13 (valine ring), and the dimethylamino group (probably protonated) interacting with hydrophilic residues located close to the serine ring (position 6). The possibility of interaction between the butylamino group of tetracaine and hydrophobic

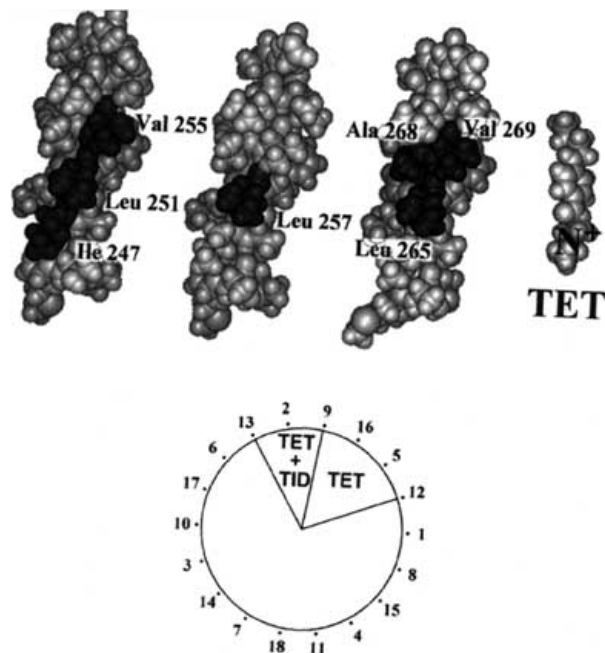


Fig. (7). **Top,** Model for tetracaine binding within the AChR ion channel in the resting state (taken from [95], with permission). Space-filling models of the α -helical M2 transmembrane domain of α 1 (Alpha), β 1 (Beta), and δ (Delta) subunits. The residues labeled by [^3H]tetracaine (shaded) lie on a single helical face. TET, Space-filling model at the same scale of the tetracaine molecule in an extended conformation where N^+ is the protonated tertiary amine. The presumed photoreactive aromatic atoms of tetracaine are positioned at the same level as the labeled residues of the M2 helices [position 9 (leucine ring)]. In this orientation, the dimethylaminoethyl group would be in proximity to the hydrophilic side chains at position 2 (threonine ring) and 6 (serine ring), whereas its *N*-butyl group is aligned with hydrophobic residues at position 12 and 13 (valine ring). **Bottom,** Helical wheel depicting the carbons of the labeled residues in the α 1 subunit (positions 5, 9, and 13) span 80° of the helix cylinder, and those of the subunit (positions 9, 12, and 13) span 100° of the helical face. Thus, identification of amino acids labeled by [^3H]tetracaine extends the definition of the surface of the M2 helices lining the lumen of the resting channel beyond those side chains labeled by [^{125}I]TID (residues 9 and 13; reviewed in [29]).

residues from position 12 and 13 is supported by the fact that procaine, which lacks the butyl group on the *N*-aryl moiety, interacts with the resting AChR with 1,000-fold lower affinity than tetracaine [70] (see Table 2). In addition, the fact that tetracaine is 10 times more potent an inhibitor of *Torpedo* than of mouse muscle AChRs, can be explained by natural substitutions found in each receptor [96]. In this regard, one of the four natural substitutions (Ser to Phe at position 6 from the α 1 subunit) decreases the polarity at position 6 (serine ring) reducing the favorability of interaction with the charged dimethylamino group of tetracaine. Figure (7; **Bottom**) shows the helical wheel depicting the carbons of the labeled residues in the α 1 subunit (positions 5, 9, and 13) span 80° of the helix

cylinder, and those of the subunit (positions 9, 12, and 13) span 100° of the helical face. Thus, the additional residues labeled by [^3H]tetracaine (Ala²⁶⁸ and Ile²⁴⁷) extend the definition of the surface of the M2 helix that is oriented toward the channel lumen in the resting (closed) state beyond those side chains labeled by [^{125}I]TID (residues 9 and 13; reviewed in [29]).

Additional pharmacological studies indicate that the binding site for the LA tetracaine in the AChR resting state overlaps with the locus for barbiturates, a class of general anesthetics [97, 98], as well as for the site of both ketamine and PCP [98], another class of general anesthetics with behavioral properties known as dissociative anesthetics. Whereas barbiturates compete for either the tetracaine or the TID binding site in a mutually exclusive manner [97], ketamine and PCP compete directly (sterically) with the tetracaine locus but allosterically with the TID site [98]. In Fig. (8) we show the mutually exclusive action between tetracaine and barbiturates. Each barbiturate inhibits [^3H]tetracaine binding [Fig. (8A)] and vice versa, tetracaine inhibits [^{14}C]amobarbital binding [Fig. (8B)] with Hill coefficients close to one, suggesting a mutually exclusive manner of competition. The relative potency of barbiturates to inhibit [^3H]tetracaine binding is: amylbarbital > amobarbital >> pentobarbital > isobarbital [Fig. (8A)]. The observed K_i for tetracaine [$0.31 \pm 0.03 \mu\text{M}$; Fig. (8B)] is nearly the same as that obtained from [^3H]tetracaine equilibrium binding experiments ($0.5 \pm 0.1 \mu\text{M}$; [70]) (see Table 2). These results suggest that in the resting AChR, the binding site for some general anesthetics overlaps with the tetracaine locus.

The location of the procaine binding site has also been studied by site-directed mutagenesis [99]. The inhibitory effect of procaine on dimethylphenylpiperazinium-evoked ion channel activity of the mouse muscle AChR was increased when the double mutant α 1Ser²⁵²Ala/ β 1Thr²⁶⁵Ala was used (see Table 9). Based on this evidence, a procaine binding site location similar to that determined for QX-222 (see previous section) is assumed. Interestingly, the same mutations did not affect the inhibitory properties of barbiturates. These results indicate that in the open channel conformation, the binding site for procaine is distinct to that for the general anesthetic barbiturates. In this regard, a general conclusion might be stated: only certain general anesthetics bind to the same locus as some LAs. However, it is necessary to take into consideration that the results from our laboratory (competitive binding of tetracaine and barbiturates, ketamine, or PCP; [97, 98]) were deduced with *Torpedo* AChRs in the resting state whereas the experiments showing differential sensitivity between procaine and barbiturates to M2 mutated-containing receptors were performed on oocyte-expressing mouse AChRs in the open conformational state [99].

Regarding the localization of the cocaine binding site, recent experimental evidence using several neuronal AChR subtypes, chimeras, and mutants, has suggested that 4Phe²⁵⁵ [valine ring (position 13)] of the α 3 4 receptor subtype (see Table 9) is structurally involved with the high-affinity (-)cocaine locus [49]. There are two possible modes of interactions: (a) one possibility is that the protonated

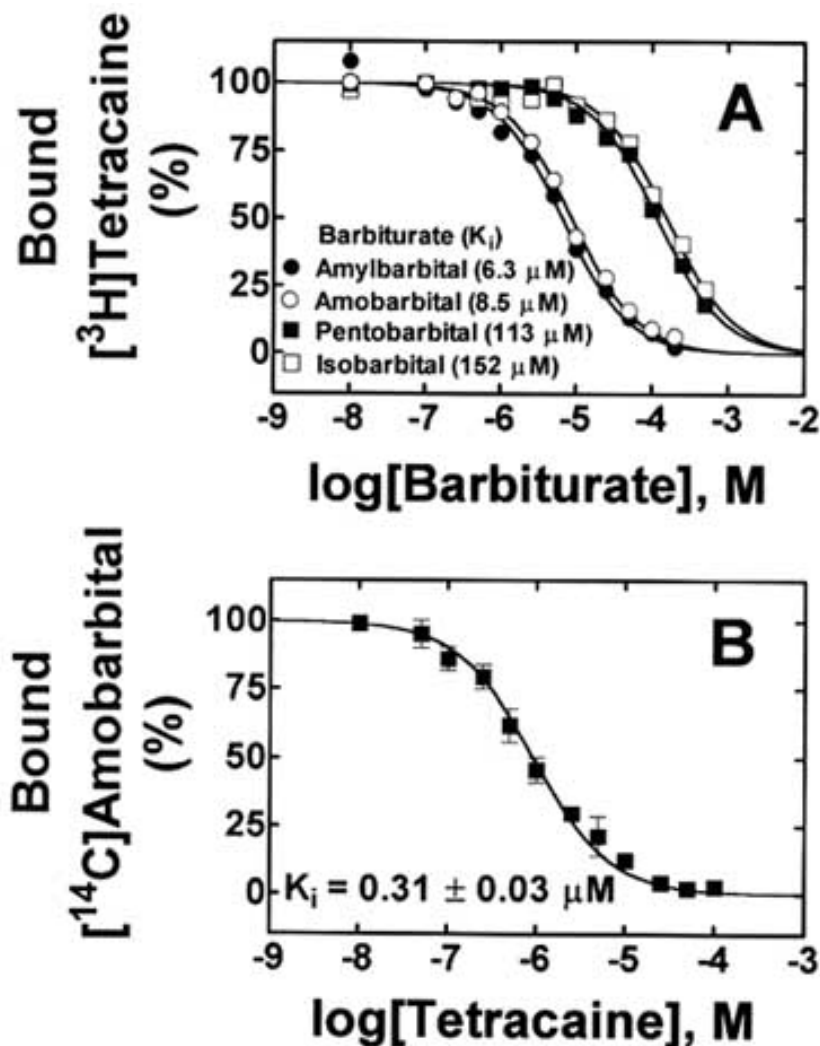


Fig. (8). Mutually exclusive action between tetracaine and barbiturates on the *Torpedo* AChR in the resting state. (A) Barbiturate-induced inhibition of [³H]tetracaine binding. AChR-rich membranes (0.2 μM) were equilibrated (1 h) with [³H]tetracaine in the presence of increasing concentrations (0.01-200 μM) of either amobarbital (○), amylbarbital (●), pentobarbital (■), or isobarbital (□). (B) Tetracaine-induced inhibition of [¹⁴C]amobarbital binding. AChR-rich membranes (0.2 μM) were equilibrated (1 h) with [¹⁴C]amobarbital in the presence of increasing concentrations (0.01-200 μM) of tetracaine. Nonspecific binding was determined in the presence of 200 μM amobarbital. The IC₅₀ value for each ligand was calculated by nonlinear least-squares fit for a single binding site. Considering that either barbiturates [97] or tetracaine [70] has one high-affinity binding site on the resting AChR, the K_i for each ligand was calculated using the observed IC₅₀ values according to the Cheng-Prusoff equation [126]: $IC_{50} = K_i / (1 + ([NCI]/K_d^{NCI}))$, where [NCI] is the initial concentration of [³H]tetracaine (11 nM) or [¹⁴C]amobarbital (7.5 μM), and K_d^{NCI} is the K_d of either [³H]tetracaine (0.5 μM; [70]) or [¹⁴C]amobarbital (3.7 μM; [97]) in the AChR resting state.

amine group of cocaine interacts with the aromatic ring of Phe by cation- interactions. In this case, the voltage-dependence of (-)cocaine inhibition (see Table 1) might arise from the electrostatic nature of the cation- interaction. The other possibility (b) is that the cocaine phenyl ring is interacting with the aromatic moiety of Phe. In this case, and considering that cocaine has a size of about 12 x 6 Å, the amine group might project deeper into the ion channel to reach position 6 (serine ring). Additional evidence suggests that (-)cocaine may allosterically inhibit the 4 2 receptor subtype by binding to a nonconserved stretch of 50 amino acids preceding the M1 domain [49].

BEHAVIORAL EFFECTS OF LOCAL ANESTHETICS

As was outlined in the Introduction, LAs, in addition to blocking nerve conduction in the peripheral nervous system, may affect the central nervous system as well. When LA molecules reach the central nervous system (e.g., after intravenous infusion and later absorption), an apparent stimulation and subsequent depression is observed (reviewed in [3]). During the stimulatory phase, symptoms such as restlessness, euphoria, muscle twitching, tremor, and clonic convulsions have been noted (reviewed in [101]). This

excitatory phase is presumably accounted for by a selective depression of inhibitory neurons (e.g., GlyR and GABA_ARs). The subsequent depression of neuronal activity causes drowsiness, sleepiness, sedation, general anesthesia, loss of consciousness, and even death by respiratory failure at high LA concentrations (reviewed in [101]). The inhibitory phase has been attributed to depressant LA actions at excitatory synapses. In this regard, both phases are presumably due solely to inhibition of neuronal activity. In addition, other behavioral effects such as dysphoria, light-headedness, visual and auditory disturbances have been considered to be elicited by LAs as well (reviewed in [101]). Interestingly, LAs, when administered systemically, suppress both neuropathic and non-neuropathic pain conditions (antinociceptive effect) in humans and animals [102-104]. In addition, procaine is believed to be the agent that precipitates panic attacks in some patients following the injection of procaine-penicillin G [105].

With the exception of (-)cocaine, LAs are not drugs of abuse, but procaine and (-)cocaine, according to their structural [see Fig. (2)] and pharmacological (see Table 2) resemblances, impart the same psychomotor stimulatory effects and function as positive reinforcers in several animal species [106, 107]. Much more important is the fact that LAs cause subjective effects in humans similar to those produced by (-)cocaine [108]. The mechanisms for the behavioral effects of LAs are poorly understood. One possibility is that LAs act, the same as (-)cocaine, on the dopamine transporter. For instance, a high correlation between LA binding affinities to the dopamine transporter and self-administration potencies in rhesus monkeys was found [109, 110]. Nevertheless, the experimental evidence described in this review pave the way to ponder on the possibility that neuronal-type AChRs, and perhaps other members of the same LGICS (e.g., 5-HT₃Rs, reviewed in [3]), are also involved in some of the pharmacological effects of LAs. Several data support such conjecture ([111, 112] and references therein): (1) both procaine and (-)cocaine antagonize the behavioral actions of nicotine in rats. For more details on the effects of nicotine in humans see the review by Willams *et al.* [113]; and (2) LAs as well as (-)cocaine produce seizures following systemic administration. Nevertheless, there is no evidence suggesting that LAs, with the exception of (-)cocaine, are involved in the mechanism of drug addiction.

CONCLUSIONS

A major focus of current research on the LGICS has been to understand the molecular mechanism of noncompetitive inhibition, and in particular, the mechanism of the action of LAs. Experimental evidence for the existence and location of both luminal (high-affinity) and nonluminal (low-affinity) LA binding sites on either muscle- or neuronal-type AChRs has been addressed in this review. The simplest mechanism to describe the action of LAs that bind to luminal sites assumes that these compounds enter the open channel, bind to different rings of amino acids within the M2 transmembrane domain, and block cation flux by sterically "plugging" the receptor pore. The existence of nonluminal

LA binding sites as well as the experimental evidence indicating that some LAs preferably bind closed ion channels, suggests additional inhibitory mechanisms. Allosteric inhibitory mechanisms can be envisioned as the structural modification of the AChR channel upon binding of one LA molecule to its specific high-affinity locus or upon binding of several LAs to its low-affinity sites at the lipid-protein interface. An allosteric inhibitory mechanism is likely to have important physiological implications as well. The LA-mediated noncompetitive inhibition of neuronal-type AChR ion channels might be important for some of the behavioral effects elicited by these drugs. Furthermore, certain LAs seem to bind to the same locus as some general anesthetics in the muscle-type AChR, indicating that certain molecular features are shared for both anesthetic classes. A better understanding of the action of LAs on AChRs as well as other members of the LGICS will be of paramount importance for the development of new drugs with therapeutic capability.

ACKNOWLEDGEMENT

This work was supported in part by NINDS Grant R29 NS35786 from the National Institute of Health (to M.P.B.). We thank Dr. Tina Machu for critical reading of the manuscript and Drs. Jonathan Cohen and Ariel Escobar for providing Figure (7) and for helping with the art-work [e.g., Fig. (5)], respectively.

REFERENCES

- [1] Catterall, W. *Adv. Neurol.*, **1999**, 79, 441.
- [2] Catterall, W. *Physiol. Rev.*, **1992**, 72, S15.
- [3] Arias, H.R. *Neurosci. Biobehav. Rev.*, **1999**, 23, 817.
- [4] Cuevas, J.; Adams, D.J. *Br. J. Pharmacol.*, **1994**, 111, 663.
- [5] Steen, P.A.; Michenfelder, J.D. *Anesthesiology*, **1979**, 50, 437.
- [6] Arias, H.R. *Neurochem. Int.*, **2000**, 36, 595.
- [7] Arias, H.R. In *Drug-Receptor Thermodynamics: Introduction and Applications*; Raffa, R.B., Ed.; John Wiley & Sons, Ltd.: USA, **2001**, Chapter 15, pp. 293-358.
- [8] Changeux, J.-P.; Edelstein, S.J. *Neuron*, **1998**, 21, 959.
- [9] Sugimoto, M.; Uchida, I.; Fukami, S.; Takenoshita, M.; Mashimoto, T.; Yoshiya, I. *Eur. J. Pharmacol.*, **2000**, 401, 329.
- [10] Hara, M.; Kai, Y.; Ikemoto, Y. *Eur. J. Pharmacol.*, **1995**, 283, 83.
- [11] Aoshima, H.; Inoue, Y.; Ueda, E.; Kitagawa, M.; Nishino, T. *J. Biochem. (Tokyo)*, **1992**, 111, 523.
- [12] Giros, B.; Caron, M.G. *Trends Pharmacol. Sci.*, **1993**, 14, 43.

- [13] Niu, L.; Abood, L.G.; Hess, G.P. *Proc. Natl. Acad. Sci. USA*, **1995**, *92*, 1208.
- [14] Ren, J.; Ye, J.H.; Liu, P.L.; Krnjevic, K.; McArdle, J.J. *Eur. J. Pharmacol.*, **1999**, *367*, 125.
- [15] Ye, J.H.; Liu, P.L.; Wu, W.H.; McArdle, J.J. *Brain Res.*, **1997**, *770*, 169.
- [16] Fan, P.; Oz, M.; Zhang, L.; Weight, F.F. *Brain Res.*, **1995**, *673*, 181.
- [17] Ortells, M.O.; Lunt, G.G. *Trends Neurosci.*, **1995**, *18*, 121.
- [18] Swope, S.L.; Moss, S.J.; Blackstone, C.D.; Haganir, R.L. *FASEB J.*, **1992**, *6*, 2514.
- [19] Mileo, A.M.; Monaco, L.; Palma, E.; Grassi, F.; Miledi, R.; Eusebi, F. *Proc. Natl. Acad. Sci. USA*, **1995**, *92*, 2686.
- [20] Mihovilovic, M.; Mai, Y.; Herbstreith, M.; Rubboli, F.; Tarroni, P.; Clementi, F.; Roses, A.D. *Biochem. Biophys. Res. Commun.*, **1993**, *197*, 137.
- [21] Anand, R.; Conroy, W.G.; Schoepfer, R.; Whiting, P.; Lindstrom, J. *J. Biol. Chem.*, **1991**, *266*, 11192.
- [22] Elgoyhen, A.B.; Vetter, D.E.; Katz, E.; Rothlin, C.V.; Heinemann, S.F.; Boulter, J. *Proc. Natl. Acad. Sci. USA*, **2001**, *98*, 3501.
- [23] McGehee, D.S.; Role, L.W. *Annu. Rev. Physiol.*, **1995**, *57*, 521.
- [24] Keyser, K.T.; Britto, L.R.G.; Schoepfer, R.; Whiting, P.; Cooper, J.; Conroy, W.; Borozozowska-Prechtel, A.; Karten, H.J.; Lindstrom, J. *J. Neurosci.*, **1993**, *13*, 442.
- [25] Palma, E.; Maggi, L.; Barabino, B.; Eusebi, F.; Ballivet, M. *J. Biol. Chem.*, **1999**, *274*, 18335.
- [26] Wang, F.; Gerzanich, V.; Wells, G.B.; Anand, R.; Peng, X.; Keyser, K.; Lindstrom, J. *J. Biol. Chem.*, **1996**, *271*, 17656.
- [27] Palma, E.; Bertrand, S.; Binzoni, T.; Bertrand, D. *J. Physiol.*, **1996**, *491.1*, 151.
- [28] Unwin, N. *Phil. Trans. R. Soc. Lond. B*, **2000**, *355*, 1813.
- [29] Arias, H.R. *Biochim. Biophys. Acta Rev. Biomembr.*, **1998**, *1376*, 173.
- [30] Jones, O.T.; McNamee, M.G. *Biochemistry*, **1988**, *27*, 2364.
- [31] Narayanaswami, V.; Kim, J.; McNamee, M.G. *Biochemistry*, **1993**, *32*, 12413.
- [32] Phillips, W.D.; Maimone, M.M.; Merlie, J.P. *J. Cell Biol.*, **1991**, *115*, 1713.
- [33] Dani, J.A. *J. Neurosci.*, **1989**, *9*, 884.
- [34] Wilson, G.G.; Karlin, A. *Neuron*, **1998**, *20*, 1269.
- [35] Auerbach, A.; Akk, G. *J. Gen. Physiol.*, **1998**, *112*, 181.
- [36] Wilson, G.G.; Karlin, A. *Proc. Natl. Acad. Sci. USA*, **2001**, *98*, 1241.
- [37] Albuquerque, E.X.; Alkondon, M.; Pereira, E.F.R.; Castro, N.G.; Schratzenholz, A.; Barbosa, C.T.F.; Bonfante-Cabarcas, R.; Aracava, Y.; Eisenberg, H.M.; Maelicke, A. *J. Pharm. Exp. Ther.*, **1997**, *280*, 1117.
- [38] Role, L.W.; Berg, D.K. *Neuron*, **1996**, *16*, 1077.
- [39] Pugh, P.C.; Berg, D.K. *J. Neurosci.*, **1994**, *14*, 889.
- [40] Messi, M.L.; Renganathan, M.; Grigorenko, E.; Delbono, O. *FEBS Lett.*, **1997**, *411*, 32.
- [41] Galzi, J.L.; Changeux, J.P. *Neuropharmacology*, **1995**, *34*, 563.
- [42] Wonnacott, S. *Trends Neurosci.*, **1997**, *20*, 92.
- [43] Jones, M.V.; Westbrook, G.L. *Trends Neurosci.*, **1996**, *19*, 96.
- [44] Dani, J.A.; Heinemann, S. *Neuron*, **1996**, *16*, 905.
- [45] De Paula, E.; Schreier, S. *Brazilian J. Med. Biol. Res.*, **1996**, *29*, 877.
- [46] Koblin, D.D.; Lester, H. *Mol. Pharmacol.*, **1979**, *15*, 559.
- [47] Neher, E.; Steinbach, J.H. *J. Physiol.*, **1978**, *277*, 153.
- [48] Charnet, P.; Labarca, C.; Cohen, B.N.; Davidson, N.; Lester, H.A.; Pilar, G. *J. Physiol.*, **1992**, *450*, 375.
- [49] Francis, M.M.; Vazquez, R.W.; Papke, R.L.; Oswald, R.E. *Mol. Pharmacol.*, **2000**, *58*, 109.
- [50] Adams, P.R. *J. Physiol.*, **1977**, *268*, 291.
- [51] Charnet, P.; Labarca, C.; Lester, H.A. *Mol. Pharmacol.*, **1994**, *41*, 708.
- [52] Charnet, P.; Labarca, C.; Leonard, R.J.; Vogelaar, N.J.; Czyzyk, L.; Gouin, A.; Davidson, N.; Lester, H.A. *Neuron*, **1990**, *2*, 87.
- [53] Leonard, R.J.; Labarca, C.G.; Charnet, P.; Davidson, N.; Lester, H.A. *Science*, **1988**, *242*, 1578.
- [54] Horn, R.; Brodwick, M.S.; Dickey, W.D. *Science*, **1980**, *210*, 205.
- [55] Gage, P.W.; Hamill, O.P.; Wachtel, R.E. *J. Physiol.*, **1983**, *335*, 123.
- [56] Swanson, K.L.; Albuquerque, E.X. *J. Pharmacol. Exp. Ther.*, **1987**, *243*, 1202.
- [57] Aracava, Y.; Ikeda, S.R.; Daly, J.W.; Brookes, N.; Albuquerque, E.X. *Mol. Pharmacol.*, **1984**, *26*, 304.
- [58] Ikeda, S.R.; Aronstam, R.S.; Daly, J.W.; Aracava, Y.; Albuquerque, E.X. *Mol. Pharmacol.*, **1984**, *26*, 293.
- [59] Aguayo, L.G.; Pazhenchevsky, B.; Daly, J.W.; Albuquerque, E.X. *Mol. Pharmacol.*, **1981**, *20*, 345.
- [60] Neher, E. *J. Physiol.*, **1983**, *339*, 663.
- [61] Ruff, R.L. *Biophys. J.*, **1982**, *37*, 625.
- [62] Dilger, J.P.; Vidal, A.M. *Mol. Pharmacol.*, **1994**, *45*, 169.

- [63] Charlesworth, P.; Jacobson, I.; Pocock, G. Richards, C.D. *Br. J. Pharmacol.*, **1992**, *106*, 802.
- [64] Niu, L.; Hess, G.P. *Biochemistry*, **1993**, *32*, 3831.
- [65] Hess, G.P.; Ulrich, H.; Breiting, H.-G.; Niu, L.; Gameiro, A.M.; Grever, C.; Srivastava, S.; Ippolito, J.E.; Lee, S.M.; Jayaraman, V.; Coombs, S.E. *Proc. Natl. Acad. Sci. USA*, **2000**, *97*, 13895.
- [66] Arias, H.R.; McCurdy, E.M.; Blanton, M.P. *Mol. Pharmacol.*, **2001**, *59*, 1051.
- [67] Heidmann, T.; Oswald, R.E.; Changeux, J.-P. *Biochemistry*, **1983**, *22*, 3112.
- [68] Arias, H.R.; Alonso-Romanowski, S.; Disalvo, E.A.; Barrantes, F.J. *Biochim. Biophys. Acta*, **1994**, *1190*, 393.
- [69] Arias, H.R. *Arch. Biochem. Biophys.*, **1999**, *371*, 89.
- [70] Middleton, R.E.; Strnad, N.P.; Cohen, J.B. *Mol. Pharmacol.*, **1999**, *56*, 290.
- [71] Horváth, L.I.; Arias, H.R.; Hankovszky, H.O.; Hideg, K.; Barrantes, F.J.; Marsh, D. *Biochemistry*, **1990**, *29*, 8707.
- [72] Earnest, J.P.; Wang, H.H.; McNamee, M.G. *Biochem. Biophys. Res. Commun.*, **1984**, *123*, 862.
- [73] Earnest, J.P.; Limbacher, H.P.; McNamee, M.G.; Wang, H.H. *Biochemistry*, **1986**, *25*, 5809.
- [74] Arias, H.R.; Sankaram, M.B.; Marsh, D.; Barrantes, F.J. *Biochim. Biophys. Acta*, **1990**, *1027*, 287.
- [75] Chattopadhyay, A.; McNamee, M.G. *Biochemistry*, **1991**, *30*, 7159.
- [76] Arias, H.R. *Biochim. Biophys. Acta*, **1997**, *1347*, 9.
- [77] Addona, G.H.; Sandermann, H.; Kloczewiak, M.A.; Husain, S.S.; Miller, K.W. *Biochim. Biophys. Acta*, **1998**, *1370*, 299.
- [78] Corbin, J.; Wang, H.H.; Blanton, M.P. *Biochim. Biophys. Acta*, **1998**, *1414*, 65.
- [79] Arias, H.R. *Mol. Membr. Biol.*, **1995**, *12*, 339.
- [80] Blanton, M.P.; Dangott, L.J.; Raja, S.K.; Lala, A.K.; Cohen, J.B. *J. Biol. Chem.*, **1998**, *273*, 8659.
- [81] González-Ros, J.M.; Farach, M.C.; Martínez-Carrión, M. *Biochemistry*, **1983**, *22*, 3807.
- [82] Krodel, E.K.; Beckman, R.A.; Cohen, J.B. *Mol. Pharmacol.*, **1979**, *15*, 294.
- [83] Neubig, R.R.; Krodel, E.K.; Boyd, N.D.; Cohen, J.B. *Proc. Natl. Acad. Sci. USA*, **1979**, *76*, 690.
- [84] Sobel, A.; Hewidmann, T.; Cartaud, J.; Changeux, J.-P. *Eur. J. Biochem.*, **1980**, *110*, 13.
- [85] Saitoh, T.; Oswald, R.; Wennogle, L.P.; Changeux, J.-P. *FEBS Lett.*, **1980**, *116*, 30.
- [86] Oswald, R.E.; Changeux, J.-P. *Biochemistry*, **1981**, *20*, 7166.
- [87] Oswald, R.E.; Changeux, J.-P. *Proc. Natl. Acad. Sci. USA*, **1981**, *78*, 3925.
- [88] Pedersen, S.E.; Sharp, S.D.; Liu, W.-S.; Cohen, J.B. *J. Biol. Chem.*, **1992**, *267*, 10489.
- [89] Husain, S.S.; Froman, S.A.; Klockzewiak, M.A.; Addona, G.H.; Olsen, R.W.; Pratt, M.B.; Cohen, J.D.; Miller, K.W. *J. Med. Chem.*, **1999**, *42*, 3300.
- [90] Pratt, M.B.; Husain, S.S.; Miller, K.W.; Cohen, J.B. *J. Biol. Chem.*, **2000**, *275*, 29441.
- [91] Bouzat, C.; Barrantes, F.J. *J. Biol. Chem.*, **1996**, *271*, 25835.
- [92] Revah, F.; Bertrand, D.; Galzi, J.-L.; Devillers-Thiéry, A.; Mülle, C.; Hussy, N.; Bertrand, S.; Ballivet, M.; Changeux, J.-P. *Nature*, **1991**, *353*, 846.
- [93] Ortells, M.O.; Lunt, G.G. *Recept. Chann.*, **1994**, *2*, 53.
- [94] Pascual, J.M.; Karlin, A. *J. Gen. Physiol.*, **1998**, *111*, 717.
- [95] Gallagher, M.J.; Cohen, J.B. *Mol. Pharmacol.*, **1999**, *56*, 300.
- [96] Eterovic, V.A.; Li, L.; Ferchmin, P.A.; Lee, Y.H.; Hann, R.M.; Rodriguez, A.D.; McNamee, M.G. *Cell Mol. Neurobiol.*, **1993**, *13*, 111.
- [97] Arias, H.R.; McCurdy, E.M.; Gallagher, M.J.; Blanton, M.P. *Mol. Pharmacol.*, **2001**, *60*, 497.
- [98] Arias, H.R.; McCurdy, E.A.; Bayer, E.Z.; Gallagher, M.J.; Blanton, M.B. *Arch. Biochem. Biophys.*, in press.
- [99] Yost, C.S.; Dodson, B.A. *Cell. Mol. Neurobiol.*, **1993**, *13*, 159.
- [100] Blanton, M.P.; Cohen, J.B. *Biochemistry*, **1994**, *33*, 2859.
- [101] Ritchie, J.M.; Green, N.M. In *The pharmacological basis of therapeutics*; Gilman, A.G.; Rall, T.W.; Nies, A.S.; Taylor, P. Eds.; New York: Pergamon Press, **1991**, pp. 311-331.
- [102] Ferrante, F.M.; Paggioli, J.; Cherukuri, S.; Arthur, G.R. *Anesth. Analg.*, **1996**, *82*, 91.
- [103] Attal, N.; Gaude, V.; Brasseur, L.; Dupuy, M.; Guirimand, F.; Parker, F.; Bouhassira, D. *Neurology*, **2000**, *54*, 564.
- [104] Rigon, A.R.; Takahashi, R.N. *Gen. Pharmacol.*, **1996**, *27*, 647.
- [105] Winter, J.T.V. *J. Pediatr.*, **1984**, *105*, 661.
- [106] Woolverton, W.L.; Balster, R.L. *Pharmacol. Biochem. Behav.*, **1979**, *11*, 669.
- [107] Zacny, J.P.; Woolverton, W.L. *Pharmacol. Biochem. Behav.*, **1989**, *33*, 527.
- [108] VanDyke, C.; Jatlow, P.; Ungerer, J.; Barash, P.; Ryck, R. *Life Sci.*, **1979**, *24*, 271.
- [109] Wilcox, K.M.; Paul, I.A.; Woolver, W.L. *Eur. J. Pharmacol.*, **1999**, *367*, 175.

- [110] Wilcox, K.M.; Rlett, J.K.; Paul, I.A.; Ordway, G.A.; Woolver, W.L. *Psychopharmacology*, **2000**, *153*, 139.
- [111] Lerner-Marmarosh, N.; Carroll, F.I.; Abood, L.G. *Life Sci.*, **1995**, *56*, 67.
- [112] Damaj, M.I.; Slemmer, J.E.; Carroll, F.I.; Martin, B.R. *J. Pharmacol. Exp. Ther.*, **1999**, *289*, 1229.
- [113] Williams, M.; Arneric, S. *Exp. Opin. Invest. Drugs*, **1996**, *5*, 1035.
- [114] Aronstam, R.S.; Eldefrawi, A.T.; Pessah, I.N.; Daly, J.W. *J. Biol. Chem.*, **1981**, *256*, 2843.
- [115] Bufler, J.; Franke, C.; Parnas, H.; Dudel, J. *Eur. J. Neurosci.*, **1996**, *8*, 677.
- [116] Dudel, J.; Schramm, M.; Franke, C.; Ratner, E.; Partnas, H. *J. Neurophysiol.*, **1999**, *81*, 2386.
- [117] Karpen, J.W.; Aoshima, H.; Abood, L.G.; Hess, G.P. *Proc. Natl. Acad. Sci. USA*, **1982**, *79*, 2509.
- [118] Karpen, J.W.; Hess, G.P. *Biochemistry*, **1986**, *25*, 17777.
- [119] Hennings, E.C.; Kiss, J.P.; De Oliveira, K.; Toth, P.T.; Vizi, E.S. *J. Neurochem.*, **1999**, *73*, 1043.
- [120] Ogden, D.C.; Siegelbaum, S.A.; Colquhoun, D. *Nature*, **1981**, *289*, 596.
- [121] Weiland, G.A.; Durkin, J.A.; Henley, J.M.; Simasko, S.M. *Mol. Pharmacol.*, **1987**, *32*, 625.
- [122] Palma, A.; Herz, J.M.; Wang, H.H.; Taylor, P. *Mol. Pharmacol.*, **1986**, *30*, 243.
- [123] Dreyer, E.B.; Hasan, F.; Cohen, S.G.; Cohen, J.B. *J. Biol. Chem.*, **1986**, *261*, 13727.
- [124] Boyd, N.D.; Cohen, J.B. *Biochemistry*, **1984**, *23*, 4023.
- [125] Blanton, M.P.; McCardy, E.; Gallaher, T.; Wang, H.H. *Mol. Pharmacol.*, **1988**, *33*, 634.
- [126] Blanchard, S.G.; Raftery, M.A. *Proc. Natl. Acad. Sci. USA*, **1979**, *76*, 81.
- [127] Cheng, Y.C.; Prusoff, W.H. *Biochem. Pharmacol.*, **1973**, *22*, 3099.